NASA Contractor Report 191186
AIAA-93–1086

# Electromagnetic Propulsion for Spacecraft

Roger M. Myers
*Sverdrup Technology, Inc.*
*Lewis Research Center Group*
*Brook Park, Ohio*

Prepared for the
1993 Aerospace Design Conference
sponsored by the American Institute of Aeronautics and Astronautics
Irvine, California, February 15–18, 1993

NASA
National Aeronautics and
Space Administration

# ELECTROMAGNETIC PROPULSION FOR SPACECRAFT

Roger M. Myers
Sverdrup Technology, Inc.
NASA Lewis Research Center Group
Brookpark, OH 44142

## Abstract

Three electromagnetic propulsion technologies, solid propellant pulsed plasma thrusters (PPT), magnetoplasmadynamic (MPD) thrusters, and pulsed inductive thrusters (PIT), have been developed for application to auxiliary and primary spacecraft propulsion. Both the PPT and MPD thrusters have been flown in space, though only PPTs have been used on operational satellites. The performance of operational PPTs is quite poor, providing only ~ 8% efficiency at ~ 1000 s specific impulse. However, laboratory PPTs yielding 34% efficiency at 2000 s specific impulse have been extensively tested, and peak performance levels of 53% efficiency at 5170 s specific impulse have been demonstrated. MPD thrusters have been flown as experiments on the Japanese MS-T4 spacecraft and the Space Shuttle and have been qualified for a flight in 1994. The flight MPD thrusters were pulsed, with a peak performance of 22% efficiency at 2500 s specific impulse using ammonia propellant. Laboratory MPD thrusters have been demonstrated with up to 70% efficiency and 7000 s specific impulse using lithium propellant. While the PIT thruster has never been flown, recent performance measurements using ammonia and hydrazine propellants are extremely encouraging, reaching 50% efficiency for specific impulses between 4000 to 8000 s. This paper reviews the fundamental operating principals, performance measurements, and system level design for the three types of electromagnetic thrusters, and available data on flight tests are discussed for the PPT and MPD thrusters.

## Introduction

Electromagnetic plasma thruster applications range from currently operational 30 W pulsed plasma thrusters (PPTs) used for satellite positioning and drag make-up to proposed 100 kW class magnetoplasmadynamic (MPD) and pulsed inductive thrusters (PIT) for robotic and piloted planetary exploration. The benefits of using electromagnetic thrusters include their ability to provide small impulse bits for satellite positioning, high specific impulse, robustness, high power processing capability, and system simplicity. While all electromagnetic thrusters rely on the interaction between a discharge current and the self-induced and/or an externally-applied magnetic field to generate thrust, the different thruster types achieve their performance goals in very different ways. In addition, their capability for pulsed operation offers the opportunity to achieve the higher performance associated with high power operation at low average power levels, permitting application of these technologies to nearer term missions. Pulsed thrusters also permit relatively simple system level scaling with available spacecraft power via changes in the thruster pulse frequency.

Like most electric propulsion systems, electromagnetic thrusters underwent an intense period of development during the 1960's and early 1970's. These efforts culminated in first flights of solid propellant pulsed plasma thrusters in the Soviet Union in 1964[1] and in the United States in 1968.[2] The Soviet PPT flight, in which the thruster provided attitude control for the Zond-2 spacecraft on its way to Mars, was the first use of electric propulsion on a planetary spacecraft. The U.S. has launched several satellites using PPTs for attitude control and drag make-up, and currently has 3 operational satellites (the NOVA series) using PPTs for high accuracy satellite positioning.[2-5] China launched its first PPT in 1981.[6] While an attempt has been made to increase the PPT power level to several hundred watts, several design problems discussed below have so far prevented this advance.[7] Other electromagnetic thrusters, however, are better suited to higher power applications. After the late 1960's, work on higher power thrusters in the United States was continued at a much reduced level, though there has recently been a resurgence of interest in the high power propulsion technologies.[8,9]

This paper is divided into three main sections, the first describing work on pulsed plasma thrusters, the second focussing on magnetoplasmadynamic thrusters, and the last addressing the status of pulsed inductive thrusters. For each thruster type the principles of operation and typical performance data are discussed first, followed by a review of flight experience and technology development requirements. Finally, a summary of the status of electromagnetic propulsion technology for spacecraft propulsion is provided.

## Pulsed Plasma Thrusters

### Principles of Operation and Typical Performance Levels

The only plasma propulsion concept currently used on U.S. satellites are solid propellant pulsed plasma thrusters. In these devices, shown schematically in Figure 1, a solid fluorinated polymer bar is inserted between two planar electrodes and an arc discharge is initiated across its face using a small ignitor electrode. The high arc current ablates a small amount of fluorinated polymer, which is then accelerated toward the exit plane by the Lorentz body force arising from the interaction of the discharge current and the induced perpendicular magnetic field. Depending on the thruster design and operating conditions, a substantial fraction of the ablated fluorinated polymer may consist of neutral atoms, and these are accelerated gas dynamically.[10]

The fluorinated polymer plasma thrusters evolved from earlier devices which utilized gaseous propellants, with high speed valves providing short bursts of propellant for acceleration.[11-13] Some of these thrusters reached a rather advanced state of system development,[14] though none ever approached flight status. A major limitation with gaseous pulsed plasma thrusters is the requirement for extremely fast, highly reliable valves. This requirement was eliminated by replacing the gaseous propellant with a solid dielectric bar, and studies in the late 1960's led to the selection of fluorinated polymer as the most appropriate propellant.

Models of PPT plasma acceleration are usually based on circuit analysis in which the rapidly moving arc is included as a variable inductance.[14,15] As shown in Figure 2, the thruster is basically a one turn inductor with the arc forming a moving conductor. The equivalent circuit for the thruster is shown in Figure 2, where $L_p$ and $R_p$ are the variable inductance and resistance arising from the moving arc. Standard circuit analysis techniques are used to predict the arc position as a function of time or arc velocity. The rapid change in inductance as the arc traverses downstream gives rise to an induced voltage drop, and a key feature of the devices is that a significant fraction of their voltage drop results from the dynamic nature of the discharge. The major difficulty of modeling the acceleration process arises during the calculation of the plasma parameters needed to predict $R_p$ and $L_p$.[15]

A typical time history of a fluorinated polymer PPT discharge is shown in Figure 3. The capacitor is first charged to over 1000 V and the discharge is initiated using a small spark plug. Following a rapid rise of discharge current to several thousand amperes, the discharge then rings as a damped oscillator, with a characteristic that depends on the circuit inductance and impedance. The peak power for the case shown exceeds 3 megawatts. These data were obtained from an early laboratory device. Flight qualified thrusters for the LES-8/9 satellites operated at a peak current of 18 kA with a total discharge duration of about 12 μs.[16]

Data obtained with a large variety of PPT geometries and circuits have been used to establish empirical performance trends.[15,17-24] Typical results are shown in Figures 4 and 5. In Figure 4 the impulse bit and specific impulse obtained using the rear-fed geometry shown in Figure 1 are plotted as a function of the energy stored in the capacitor. While both the impulse bit, defined as the total impulse delivered per thruster discharge, and specific impulse generally increase with capacitor energy, the degree of scatter in the specific impulse is quite large. Peak specific impulse for the discharge energy range shown in Figure 4 is 400 s. Figure 5 shows data for a side-feed PPT with flared electrodes. The energy was increased to 20 J/shot, and the specific impulse increased to a peak of 1400 s. Thruster performance was varied by changing the spacing between two fluorinated polymer propellant faces in the discharge chamber.[17] The increased propellant surface area exposed to the arc with a side-feed configuration was

found to significantly increase the ablated propellant mass per discharge over that obtained with the rear feed configuration, resulting in a higher impulse bit, but reducing the specific impulse for a given discharge energy. This effect was dramatically shown by Palumbo and Guman,[21] who showed that simply changing from a side-feed to a rear-feed geometry at a constant discharge energy of 450 J increased the specific impulse from 1280 to 5170 s, and raised the efficiency from 23% to 53%.

Other fluorinated polymer PPT studies examined the influence of electrode length, width, shape, propellant geometry, the use of external magnetic fields, and choice of electrode material. Of particular importance, increasing the electrode lengths from 7 cm to 17 cm increased the thruster efficiency from 26 to 35% for a side-feed thruster with a discharge energy of 750 J.[22] PPT models have been used to establish performance trends for simple parallel rail electrode geometries,[15] but no first-principles analysis of PPTs has been performed. For instance, the proportionality between impulse bit magnitude and the stored energy is well predicted, but the quantitative relationship is very sensitive to the effects of field-fringing at the accelerator side-walls and the initial plasma conditions.[15] Neither of the latter are easily accounted for in the models. The models also correctly predict the behavior of mass ablated/shot, specific impulse, and efficiency with circuit parameters for the simple rear-fed designs with parallel electrodes.

The introduction of applied magnetic fields was also found to significantly improve PPT performance.[19,24] Figure 6 shows a schematic of an applied-field PPT, and Figure 7 shows that increasing the applied-field strength from 0 to 0.3 T resulted in a specific impulse increase of almost a factor of three and a half and an efficiency increase from 20% to 34% for this thruster design. However, a corresponding decrease in the ablated mass/shot decreased the impulse bit. The increased accelerating magnetic field appears to have decreased the arc residence time near the fluorinated polymer surface, which decreased the heat flux to the propellant and resulted in the observed decrease in mass/shot. No predictive model exists which includes the effects of the applied magnetic fields.[19]

PPT lifetime has been studied via a series of lifetests. Thruster system demonstrations have exceeded $10^7$ pulses for flight qualification.[3,16,25-27] No thruster life limitations were reported for the early flight systems with discharge energies of a few joules, but when an attempt was made to scale up to several hundred joules per discharge the copper anode was found to erode severely near the thruster exit plane.[22] Surface analysis indicated the problem was local melting of the anode material. Extensive materials testing resulted in the data listed in Table 1, which show that graphite and copper have the lowest erosion rates for a given configuration, though the difference between them was not large enough to solve the problem.[22] The problem was ultimately resolved by increasing the electrode length by over a factor of two, leading to a reduction of the arc residence time at the exit plane. It appears that increasing the discharge energy, with the resultant increase in arc velocity, caused the arc to reach the end of the electrodes before the capacitors had fully discharged. This increased the arc residence time at the thruster exit plane. For the short electrode configuration the arc should have traversed the electrodes in approximately 5 μs, so that it is not surprising that the 30 μs discharge[28] caused significant erosion. A similar phenomenon has been carefully documented for gaseous pulsed accelerators when the current pulse duration exceeded the time required for the arc to traverse the electrode length.[29]

Pulsed Plasma Thruster Flight Experience

There is an extensive data base of flight and flight-qualification experience for solid propellant pulsed plasma thrusters.[2-5,16,25-27,30,31] Shown in Figure 8 is a plot of impulse bit vs. discharge energy for some of the major space test programs. Of those shown, L-4SC-3 and ETS-IV were Japanese flights, MDT-2A was Chinese, LES-9 and SMS (Synchronous Meteorological Satellite) were U.S. satellites which were flight qualified but not flown, and the side-feed PPTs, developed principally in the U.S., never reached full flight-qualification. The LES-6 mission, launched in 1968, lasted for 5 years during which the four PPT thrusters on the spacecraft delivered a total of $6.8 \times 10^7$ pulses with impulse bits of 26.8 μN-s. The three NOVA spacecraft, launched between 1981 and 1985, are currently in use as part of the U.S. Navy's TRANSIT navigation satellite series.[5]

A typical PPT flight system schematic is shown in Figure 9. The particular case shown is that for the Chinese

MDT-2A flight. The power conditioner controls the charging of both the ignitor and energy storage capacitors, and once charging is complete the controller sends a firing signal to the ignitor. The energy storage capacitor discharges as soon as the conductivity between the thruster electrodes increases to a high enough value. As shown in Figure 1, a negator spring forces the fluorinated polymer propellant up against a step on one of the thruster electrodes.

Figures 10 and 11 show a component level breakdown and an assembled PPT used on the NOVA spacecraft series.[4] The fluorinated polymer propellant bar had a V-groove cut in the exposed face (90 degree included angle) to increase the propellant surface area subject to the accelerating arc. In addition to satisfying the thruster performance requirements, the thruster housing and nozzle exit designs were constrained by electromagnetic interference (EMI) and spacecraft contamination considerations. These issues are further discussed below. The NOVA spacecraft provides approximately 30 W of power to the PPT system, and each thruster discharge uses approximately 45 μg of fluorinated polymer to provide a 0.374 mN-s impulse bit. The fluorinated polymer propellant bar is sized to provide approximately $1.3 \times 10^7$ discharges, yielding a total impulse of about $4.5 \times 10^3$ N-s over the 10 year design lifetime. A flight PPT system with a total impulse capability of 7320 N-s per thruster was developed for the LES-8/9 spacecraft.[16] The LES-8/9 thrusters were fully flight qualified but were never flown.[16]

Electromagnetic interference (EMI) induced by the high voltage and current transients during the thruster discharge was the most serious problem encountered during PPT qualification testing.[5,30,32,33] While considerable effort was expended to eliminate EMI on the early LES-6 flight, even the first NOVA satellite, launched 13 years later, experienced a gradual onset of EMI induced problems. The investigation leading to a solution for the NOVA spacecraft is described in detail by Ebert et al.,[5] where it was found that simple modifications of the grounding circuitry resulted in large reductions in radiated EMI. Other EMI experiences with all types of electric propulsion systems are reviewed by Sovey et al.[33]

The second major integration issue was spacecraft contamination by the thruster exhaust. While this was not considered a significant issue with the early low energy discharges,[34] considerable effort went into quantifying the plume characteristics for the higher energy thrusters.[31,34-36] Using a variety of diagnostics, ranging from high speed photography to mass spectroscopy, it was found that the PPT plume consisted predominantly of neutral atoms, with ionization fractions below 10%. Plume species include atomic carbon, fluorine, hydrogen, oxygen, and a variety of molecular species.[31] Deposition measurements made using quartz-crystal microbalances in the Molecular Sink Facility at JPL showed that the original thruster nozzle design yielded considerable deposition of exhaust products on surfaces upstream of the thruster exhaust.[34] Increasing the nozzle expansion half-angle from the original 15° to 30° to expand the neutral plume constituents to a lower pressure resulted in up to a factor of two reduction in backflow.[34]

Pulsed Plasma Thruster Technology Requirements

With the advent of new low-power, low-mass satellite constellations there is potential for application of PPTs to drag make-up, attitude control, and even primary propulsion functions in low-Earth orbit.[37] Their capability of providing a wide range of thruster performance by simply changing the geometry of the propellant surface exposed to the arc discharge is apparently unique. In addition, recent developments in plastics technologies may further expand the performance capabilities of PPTs and permit system simplifications for higher total impulse missions. However, for higher power PPTs to become competitive with other propulsion technologies, improvements must be demonstrated in capacitor technology, system reliability, and high performance thruster lifetime.[7] The major problems experienced during the course of higher power PPT development were capacitor failure, propellant feed jamming, uneven erosion of the propellant, and insulator breakdown between the capacitor and thruster assembly.[7] While many of these problems have been resolved,[7,38] the application of PPTs to low-power spacecraft requires demonstration of a long life, high performance thruster. Substantial performance improvements have been demonstrated in the laboratory by changing the propellant geometry,[21] increasing the electrode length,[22] or applying external magnetic fields.[19] However, the system level implications of these changes have not been studied. Thus, while improvements have been demonstrated, no consistent performance and lifetime data base exists at higher discharge energies, and ultimate performance limits have not been established.

## Magnetoplasmadynamic Thrusters

In addition to PPTs, MPD thrusters are the only other electromagnetic propulsion device which has flown in space. These thrusters operate on the same general principles as pulsed plasma thrusters, though the discharge duration is sufficiently long for the current and plasma flow to reach a steady-state distribution, which usually occurs within 200 μs. MPD thrusters are operated either steady-state for several hours at a time or quasi-steady, in which the discharge is pulsed for 1 to 10 ms at a frequency determined by the peak instantaneous power and the available spacecraft power. Only quasi-steady MPD thrusters have flown. Two recent reviews have been written about MPD thruster technology. The first, by Sovey and Mantenieks,[8] covers experimental performance and lifetime studies until 1987. The second, by Myers, Mantenieks, and LaPointe[9] covers both experimental and modeling efforts through 1991.

A typical applied-field MPD thruster is shown in Figure 12. Self-field thrusters are similar in design, but do not include the external magnet coil. Gaseous propellant is injected through an insulator at the rear of the chamber, and an arc is struck between the anode and cathode using a high voltage ignitor supply. The Lorentz force resulting from the interaction between the stationary discharge current and the self-induced $B_\theta$ and externally applied $B_r$ and $B_z$ magnetic fields accelerates the resulting plasma. Two force components arise from the self-induced field, an axial force due to the $j_r B_\theta$ interaction, and a compressive force due to the $j_z B_\theta$ interaction. Use of an applied magnetic field gives rise to additional accelerating terms, including azimuthal acceleration which spins the plasma, and both radial and axial force terms involving the azimuthal current induced by the presence of pressure and magnetic field gradients. The azimuthal momentum is partially converted to thrust in the diverging magnetic field downstream of the exit plane.

Only self-field MPD thruster acceleration has been successfully modeled analytically. Performing a volume integral of the J x B force terms yields[14]

$$T=\frac{\mu_0 J^2}{4\pi}\left(\ln\frac{R_a}{R_c}+K\right) \qquad (1)$$

where J is the discharge current, $R_a$ and $R_c$ are the anode and cathode radii, and K is a constant between 0.5 and 0.75 which depends on the current distribution on the electrode surfaces. This equation does not include contributions from gas dynamic expansion. More sophisticated numerical MHD codes have shown that gas dynamic expansion is important at low currents or high propellant flow rates in self-field thrusters,[39-42] though these regimes are usually associated with specific impulses below 1500 s. The self-field thruster discharge voltage has yet to be accurately modeled. This in large part reflects neglect of the electrode region,[39,43,44] though anomalous resistivity arising from plasma instabilities appears to play a role.[45,46] Recent numerical studies have also evaluated the impact of thruster lifetime requirements resulting from cathode current emission constraints on thruster performance limits.[47]

Models for applied-field MPD thrusters have not been nearly as successful as those for self-field devices. Very few have been published,[48-51] and all have relied on severe assumptions about the plasma ionization state and transport properties. Comparisons with experimental thrust measurements have shown substantial disagreement between measured values and predictions.[51,52] An effort is currently underway to develop an improved numerical MHD code incorporating applied-field effects,[53] and initial results are encouraging.

A great deal of experimental data has been collected with both self-field and applied-field MPD thrusters. Major results include performance scaling with thruster geometry, discharge current level, applied magnetic field strength, and propellant type and flow rate.[54-58] A summary of recent MPD thruster performance measurements is given in Figures 13 through 16. Data obtained at power levels over 600 kW came from quasi-steady tests. Thruster efficiency is shown as a function of specific impulse and power level in Figures 13 and 14, respectively. The highest performance was obtained with lithium propellant at 70% efficiency and 5000 s specific impulse.[8,59] While

extensive testing with lithium was done in the 1960's and early 1970's, the work was terminated due to budgetary cutbacks. It is clear that the applied-field thrusters have consistently shown higher efficiency and specific impulse than the self-field thrusters.[57,58,60] There is also a trend toward increasing efficiency as a function of discharge power, though this is not true for the specific impulse (Figure 15). Figure 16 shows a comparison of performance levels for argon and hydrogen propellants with a steady-state applied-field thruster operated at power levels between 20 and 85 kW. While the shape of the curves is the same, using hydrogen greatly extended the operating range and performance.

In addition to the performance measurements, considerable success has been achieved in the identification of major efficiency loss mechanisms and the causes of unstable thruster operation. For both self-field and applied-field MPD thrusters the dominant loss mechanism is power deposition to the anode.[57,61,62] For current thruster designs it varies between 30% and 90% of the thruster input power. The anode power fraction has been shown to decrease with both increasing power and applied magnetic field strength. Recent work has also established that the applied-magnetic field shape has a large impact on anode power deposition.[63,64] Other major losses include propellant dissociation and ionization, cathode heating, and plume divergence.[43]

MPD thruster lifetime limiters have been examined for both quasi-steady and steady-state thrusters. The longest quasi-steady thruster lifetests have lasted over $3 \times 10^6$ pulses for a total impulse of approximately $7.3 \times 10^4$ N-s.[65] The major life limiter for quasi-steady thrusters is cathode erosion, which can be as high as 20 μg per coulomb of charge transferred through the cathode.[66] Testing in Japan has revealed that use of low work function cathode materials reduces this to approximately 0.6 μg/C.[65] Steady-state thrusters have been tested at 30 kW for 500 hours using ammonia propellant, yielding a total impulse of $1 \times 10^6$ N-s,[67] and at 100 kW for 50 h using hydrogen propellant, yielding a total impulse of $5 \times 10^4$ N-s.[68] Steady-state MPD thruster lifetests have revealed that cathode erosion is very sensitive to propellant purity and the ambient pressure at the cathode surface,[9] and recent tests have examined the possibility of using hollow cathodes.[69] A recent 60 kW lifetest using argon propellant failed after 30 hours as a result of copper anode sputtering by the high speed propellant atoms.[70] For specific impulses over approximately 1500 s the energy of argon ions or atoms exceeds the sputter threshold energy of the copper anode. This problem can be solved by restricting the choice of propellants to light gases such as hydrogen, deuterium, or lithium. The lower atomic mass for these propellants reduces the particle energy to values below the anode sputtering threshold for specific impulses of interest.

Magnetoplasmadynamic Thruster Flights

The first major MPD thruster flight test occurred in 1980 on the Japanese MS-T4 spacecraft.[71,72] The thrusters were mounted so as to generate torque on the spacecraft and permit measurement of the thruster impulse bit via changes in the satellite spin rate. The thruster, shown schematically in Figure 17, included an applied-magnetic field and the anode was segmented to permit rapid diffusion of the applied-field into the discharge region. The thruster cathode was a hollow tungsten tube through which the ammonia propellant was injected. The discharge was ignited using a small trigger circuit consisting of a 2 μF capacitor charged to 3 kV, which was connected to an electrode inserted between the main thruster electrodes. The peak discharge current and voltage were 700 A and 150 V, respectively, yielding a peak power of approximately 100 kW. Each thruster discharge lasted 1.5 ms, consumed a total energy of about 200 J, and generated an impulse bit of approximately 0.7 mN-s. The instantaneous thruster performance was 22% efficiency at 2500 s specific impulse, though the system level performance was degraded by having a propellant pulse which was 4 times as long as the discharge. The MPD thruster system configuration is shown in Figure 18. The power conditioning unit contains elements for the trigger circuit, the main capacitor bank charging unit, the fast acting valve (FAV), and heaters for the ammonia propellant and valves. The FAV controls the propellant flow to the thruster. The ammonia propellant feed system contains a filter, orifice block, and shut-off valve, where the first two items were required to ensure that only gaseous ammonia reaches the FAV. During the flight the MPD thruster system was successfully operated for over 5 hours and accumulated over 400 discharges. While some problems were experienced during the flight experiment with thruster misfirings, it did successfully demonstrate operation of quasi-steady MPD thrusters in space.

The second MPD thruster flight test involved using a thruster as a plasma source to study charging of the Space Shuttle.[73-77] This experiment, part of the Space Experiment with Particle Accelerator (SEPAC) series, was launched in 1983 into a 245 km orbit as part of Spacelab 1. While the system elements were the same as for the earlier flight, their configuration and qualification testing were changed significantly to accommodate the requirements for mounting on a manned spacecraft. The MPD thruster system and operating conditions were selected on the basis of the spacecraft charging experiment requirements, and not on the system's potential propulsion applications.[78] For the SEPAC test, the external magnetic field was eliminated from the thruster design and the propellant was changed to argon gas. The placement of the SEPAC assembly on the Shuttle Spacelab pallet is shown in Figure 19, and the internal configuration is shown in Figure 20. The Neutral Gas Plume experiment (NGP) shown in Figure 20 was not part of the MPD thruster test, but was mounted on the same structure for convenience. System testing, including thermal, structural, electronic, and EMI, is described in detail by Ijichi et al.[77] and Kuriki.[73] Because the goals of the flight test were to study orbiter charging as a function of electron beam current and MPD thruster plasma injection, no attempt was made to accumulate thruster firings or measure the in-space impulse bit.[78] A total of only 20 MPD thruster firings were accumulated, each discharging a total of 2 kJ at a peak power of almost 2 MW (8000 A and 240 V). Nevertheless, the SEPAC test successfully demonstrated the operation of a high peak power MPD thruster system on the Space Shuttle.

Another Japanese flight test of an MPD thruster system for propulsion application is planned for launch on the new H-II launch vehicle in 1994.[79] Known as the Electric Propulsion Experiment (EPEX) on the Space Flyer Unit (SFU), the MPD thruster will utilize hydrazine propellant in a self-field thruster operated at peak power levels of 2 MW. The effort is part of the ongoing Japanese effort to develop a propulsion system which can be easily scaled to a variety of spacecraft power levels and mission requirements.[78] The primary experiment goals are to demonstrate operation of an MPD thruster propulsion system which comes close to matching operational requirements, and to verify ground based performance data. While the original propulsion system power was quoted as 1.25 kW, launch vehicle constraints have since reduced this to 430 W, with commensurate decreases in propulsion system performance. At present, the system specific impulse is only 600 s due to the decrease in discharge duration from 1 ms to 150 μs, which decreased the fraction of the injected propellant accelerated by the discharge to about 50% of the total injected propellant.[78] When more power becomes available for propulsion, the system performance will be improved by increasing the discharge duration. To date the complete system has been tested to 3 million pulses, and thermal, structural, and EMI compatibility has been verified.[65,80-86]

MPD Thruster Technology Requirements

The major issues currently preventing the application of MPD thrusters to primary propulsion applications are low thruster efficiency, available spacecraft power, and spacecraft integration. While adequate thruster efficiency has been demonstrated with lithium, use of condensable propellants is likely precluded on near-term, low-power spacecraft due to the potential for spacecraft contamination. The highest non-condensable propellant performance for current thruster designs is below 40%, though high power pulsed devices are showing evidence of significantly improved performance when operated using hydrogen and deuterium propellants.[65,87]

Many analyses have been done for MPD thruster propulsion systems. These range from steady-state multi-megawatt propulsion systems for manned Mars missions[88] to quasi-steady 100 kW class systems for planetary exploration.[89] Near-term applications will likely be on spacecraft with between 10 and 50 kW power levels for propulsion, for which demonstrated steady-state thruster efficiency to date is below 25%. This limitation can be overcome by either identifying improved thruster designs or by adopting the quasi-steady thruster approach used by the Japanese. If the latter approach is taken, significant improvements in capacitor and valve technologies are needed for MPD thrusters to successfully compete with alternative electric propulsion technologies.

## Pulsed Inductive Thrusters

Pulsed inductive thrusters (PITs) have been developed in the hope of eliminating thruster lifetime concerns by relying on induction of plasma currents rather than current conduction through electrode surfaces. A photograph of a current PIT design is shown in Figure 21, and schematic diagrams of the thruster operation are shown in Figures 22a and 22b. The thruster consists of a flat spiral drive coil covered by a thin insulator with a propellant distribution nozzle extending out from the center of the coil. As shown in Figure 22, a propellant pulse generated from a high speed valve is injected from the nozzle onto the drive coil surface and a high current pulse, generated by a small capacitor bank, is passed through the coil. The current transient induces a rapidly changing magnetic field in the propellant, which results in a high azimuthal electric field. The propellant breaks down and a high azimuthal current is generated in the resulting plasma. The Lorentz force between the azimuthal current and the magnetic field accelerates the plasma axially away from the coil. It is proposed that using PIT thrusters will permit use of any gas as propellant, since issues of material oxidation and chemical attack are eliminated by the inductive nature of the discharge.[90]

While PITs have never flown in space, recent experimental and theoretical results have been very encouraging. Work began on these thrusters in the late 1960's with small, 20 cm diameter coils,[91] and over the next decade increased in size to the current 1 m diameter thruster.[92] During this period a simple circuit model was developed which predicted the scaling of thruster performance with coil size and circuit parameters.[92] The PIT circuit and the modeled equivalent circuit, are shown in Figure 23. The model incorporates the effects of plasma formation and resistivity via the input parameters, which include the initial gas density distribution on the coil surface, the plasma resistivity, and the initial plasma current sheet thickness. The thruster has been extensively studied experimentally over a wide range of operating conditions, and model input parameters reflect the results of these measurements.[90-95]

Direct performance measurements made over the last year using a PIT with an improved drive circuit have shown dramatic improvements in efficiency.[90,95] Some of the results are shown in Figures 24 and 25, which show the efficiency - specific impulse characteristics for the PIT thruster operated on ammonia and hydrazine. These data were obtained by charging the PIT capacitor bank to a constant voltage and varying the propellant pulse mass via changes in the pressure on the high speed valve. Scatter in the data is the result of seismic pick-up in the thrust balance. For each case the efficiency is approximately constant for the entire range of specific impulse shown, with results for ammonia near 50% efficiency for both charging voltages (Figure 24a and 24b), and slightly over 40% for hydrazine (Figure 25). This is the only thruster type for which a nearly constant efficiency has been obtained over more than a factor of two change in specific impulse.

### Pulsed Inductive Thruster Technology Requirements

With the demonstration of high efficiency and specific impulse, the pulsed inductive thruster has overcome a major obstacle to its application to primary spacecraft propulsion. While preliminary lifetime and system level analysis has been done,[95] considerably more detail is required in these studies for an appropriate trade study to be performed. It is likely that the large thruster size required to provide high efficiency will limit application of the PIT to power levels over several kilowatts, though uncertainties in the system weight preclude identification of a minimum power level. Approximately $10^5$ discharges have been accumulated on the 1 m diameter thruster,[95] whereas missions will probably require between $10^9$ and $10^{11}$ discharges. Spectral studies have revealed the presence of silica in the plume,[95] indicating that the coil insulator may be eroding at a low level. Such results must be quantified to establish thruster lifetime. In addition, the magnitude and severity of electromagnetic interference arising from the thruster has not been addressed. EMI could be particularly severe with the PIT due to the extremely large current and voltage transients during the discharge. While adequate high-voltage capacitor technology appears to have been demonstrated, the high speed propellant valve recently failed after $10^6$ pulses, and design modifications have been proposed.[95]

## Summary

The operation and status of electromagnetic pulsed plasma, magnetoplasmadynamic, and pulsed inductive thrusters were reviewed. Pulsed plasma thrusters, which provide high specific impulse and a small impulse bit, are currently used on several U.S. and international spacecraft for drag make-up and attitude control, and are the only electric propulsion technology to have been used on an interplanetary spacecraft. Pulsed plasma thrusters have undergone extensive development and flight qualification testing, and PPTs yielding 34% efficiency at 2000 s specific impulse have reached a high state of system development. Peak demonstrated laboratory model PPT performance is 53% efficiency at 5170 s specific impulse. MPD thrusters yielding 70% efficiency at 7000 s specific impulse using lithium propellant, and 40% efficiency at 3500 s specific impulse using hydrogen propellant, have been demonstrated in laboratory tests. Quasi-steady magnetoplasmadynamic thrusters have been flown once on a Japanese spacecraft and once on the Space Shuttle. Quasi-steady MPD thruster system performance is currently limited by the available spacecraft power. A wide variety of steady-state MPD thrusters, in both self- and applied magnetic field configurations, have been tested at power levels up to several hundred kilowatts. Direct performance and lifetime measurements indicate that the best MPD thruster propellants are hydrogen, deuterium, and lithium. Pulsed inductive thrusters have recently been demonstrated with 50% efficiency for specific impulses between 4000 and 8000 s, levels which may make them an attractive alternative for primary propulsion applications. Technology requirements for all pulsed propulsion technologies include improved capacitors, high speed reliable propellant valves, and improved component designs yielding longer thruster lifetimes.

## References

1. Zhurin, V.V., "Electric Propulsion in the USSR," AIAA Paper 76-1073, November 1976.

2. Braga-Illa, A., "Preliminary Report on the Orbital Operation of the Automatic Stationkeeping System of LES-6," AIAA Paper 69-934, August 1969.

3. Vondra, R.J., "The MIT Lincoln Laboratory Pulsed Plasma Thruster," AIAA Paper 76-998, November 1976.

4. Brill, Y., Eisner, A., and Osborn, L., "The Flight Application of a Pulsed Plasma Microthruster; The Nova Satellite," AIAA Paper 82-1956, November 1982.

5. Ebert, W.L, Kowal, S.J., and Sloan, R.F., "Operational Nova Spacecraft Teflon Pulsed Plasma Thruster System," AIAA Paper 89-2497, July 1989.

6. An, S., Wu, H., Feng, X., and Liu, W., "Space Flight Test of Electric Thruster System MDT-2A," Journal of Spacecraft and Rockets, Vol., 21, No. 6, November - December 1984, pp. 593-594.

7. Cassady, R.J., " Pulsed Plasma Mission Endurance Test," Rocket Research Co., Final Report for the Period Sept. 1984 to July 1989, Air Force Astronautics Laboratory, AFAL-TR-88-105, August 1989.

8. Sovey, J.S. and Mantenieks, M.A., "Performance and Lifetime Assessment of Magnetoplasmadynamic (MPD) Arc Thruster Technology," Journal of Propulsion and Power, Vol. 7, No. 1, January-February 1991, pp. 71-83.

9. Myers, R.M., Mantenieks, M.A., and LaPointe, M.R., "MPD Thruster Technology," AIAA Paper 91-3568, September 1991, see also NASA TM 105242.

10. Vondra, R.J., Thomassen, K.I., and Solbes, A., "Analysis of Solid Teflon Pulsed Plasma Thruster," Journal of Spacecraft and Rockets, Vol. 7, No. 12, December 1970, pp. 1402-1406.

11. Larson, A.V., et al., "An Energy Inventory in a Coaxial Plasma Accelerator Driven by a Pulse Line Energy Source, AIAA Journal, Vol. 3, No. 5, May 1965, p. 977.

12. Ashby, D., Gooding, T.J., Hayworth, B., and Larson, A., "Exhaust Measurements on the Plasma From a Pulsed Coaxial Gun," AIAA Journal, Vol.3, No. 6, June 1965, pp. 1140-1142.

13. Michels, C.J., et al., "Analytical and Experimental Performance of Capacitor Powered Coaxial Plasma Guns, AIAA Journal, Vol. 4, No. 5, May 1966, p. 823.

14. Jahn, R. G., The Physics of Electric Propulsion, McGraw-Hill, 1968.

15. Solbes, A. and Vondra R. J., "Performance Study of a Solid Fuel-Pulsed Electric Microthruster," Journal of Spacecraft and Rockets, Vol. 10, No. 6, June 1973, pp. 406-410.

16. Vondra, R.J. and Thomassen, K.I., "Flight Qualified Pulsed Electric Thruster for Satellite Control," Journal of Spacecraft and Rockets, Vol. 11, No. 9, September 1974, pp. 613 - 617.

17. Vondra, R.J. and Thomassen, K.I., "Performance Improvements in Solid Fuel Microthrusters," Journal of Spacecraft and Rockets, Vol. 9, No. 19, October 1972, pp. 738 - 742.

18. Vondra, R. J., "One Millipound Pulsed Plasma Thruster Development," AIAA Paper 82-1877, November 1982.

19. Takegahara, H., Ohtsuka, T., and Kimura, I., "Effect of Applied Magnetic Fields on a Solid-Propellant Pulsed Plasma Thruster," IEPC Paper 84-50, International Electric Propulsion Conference, Tokyo, Japan, May 1984.

20. Paccani, G., "Anode Nozzle Experimental Analysis in a Coaxial Non-Steady Solid Propellant MPD Thruster," IEPC Paper 88-076, International Electric Propulsion Conference, Garmish-Partenkirchen, Germany, October 1988.

21. Palumbo, D.J. and Guman, W. J., "Effects of Propellant and Electrode Geometry on Pulsed Ablative Plasma Thruster Performance," AIAA Paper 75-409, March 1975.

22. Palumbo, D.J., "Solid Propellant Pulsed Plasma Propulsion System Development for N-S Stationkeeping," AIAA Paper 79-2097, October 1979.

23. Yuan-Zhu, K., "Effects of Propellant Geometry on PPT Performance," IEPC Paper 84-94, International Electric Propulsion Conference, 17th International Electric Propulsion Conference, Tokyo, Japan, May 1984.

24. Kimura, I., Ogiwara, K., Takegahara, H., and Suzuki, Y., "Effect of Applied Magnetic Fields on a Solid-Propellant Pulsed Plasma Thruster," AIAA Paper 79-2098, October 1979.

25. Guman, W.J. and Nathanson, D. M., "Pulsed Plasma Microthruster Propulsion System for Synchronous Orbit Satellite," Journal of Spacecraft and Rockets, Vol. 7, No. 4, April 1970, pp. 409-415.

26. Guman, W. J., "Task 4 - Engineering Model Fabrication and Test Report," Interim Task Report by Fairchild Industries, NASA contract NAS5-11494, August 1972.

27. Guman, W.J. and Williams, T.E., "Pulsed Plasma Microthruster for Synchronous Meteorological Satellite (SMS), AIAA Paper 73-1066, October 1973.

28. Vondra, R.J., "U.S. Air Force Programs in Electric Propulsion," AIAA Paper 79-2123, October 1979.

29. Eckbreth, A. C., "Current Pattern and Gas Flow Stabilization in Pulsed Plasma Accelerators," Ph.D. Dissertation, Dept. of Aerospace and Mechanical Sciences, Princeton University, December 1968.

30. Dolbec, R.E., "RFI Measurements on a LES-7 Prototype Pulsed Plasma Thruster," Journal of Spacecraft and Rockets, Vol. 7, No. 7, July 1970, pp. 889 - 890.

31. Hirata, M. and Murakami, H., "Exhaust Gas Analysis of a Pulsed Plasma Engine," IEPC Paper 84-48, 17th International Electric Propulsion Conference, Tokyo, Japan, May 1984.

32. Thomassen, K.I., "Radiation from Pulsed Electric Thrusters," Journal of Spacecraft and Rockets, Vol. 10, No. 10, October 1973, pp. 679-680.

33. Sovey, J.S., Carney, L. M., and Knowles, S.C., "Electromagnetic Emissions Experiences Using Electric Propulsion Systems - A Survey," Journal of Propulsion and Power, Vol. 5, No. 5, September - October 1989, pp. 534 - 547.

34. Rudolph, L.K. and Jones, R.M., "Pulsed Plasma Thruster Contamination Studies," AIAA Paper 79-2106, October 1979.

35. Thomassen, K.I., and Vondra, R.J., "Exhaust Velocity Measurements of a Solid Teflon Pulsed Plasma Thruster," Journal of Spacecraft and Rockets, Vol. 9, No. 1, January 1972, pp. 61-62.

36. Thomassen, K.I. and Tong., D., "Interferometric Density Measurements in the Arc of a Pulsed Plasma Thruster," Journal of Spacecraft and Rockets, Vol. 10, No. 3, March 1973, pp. 163 - 164.

37. Lorenz, R., "Small Satellites and Electric Propulsion - A Review," Aeronautical Journal, June/July 1991, pp. 204 - 213.

38. Vondra, R.J., Private Communication, Air Force Phillips Laboratory, January 1993.

39. LaPointe, M.R., "Numerical Simulation of Self-Field MPD Thrusters," AIAA Paper 91-2341, June 1991, see also NASA CR-187168.

40. Martinez-Sanchez, M., "Structure of Self-Field Accelerated Plasma Flows," Journal of Propulsion and Power, Vol. 7, No. 1, January - February 1991, pp. 56-64.

41. Sleziona, P.C., Auweter-Kurtz, M., and Schrade, H.O., "Numerical Codes for Cylindrical MPD Thrusters," IEPC Paper 88-038, 20th International Electric Propulsion Conference, Garmisch-Partenkirchen, Germany, October 1988.

42. Auweter-Kurtz, M., Glaser, S.F., Kurtz, H.L, Schrade, H.O., and Sleziona, P.C., "An Improved Code for Nozzle Type Steady State MPD Thrusters," IEPC Paper 88-040, 20th International Electric Propulsion Conference, Garmisch-Partenkirchen, Germany, October 1988.

43. Myers, R.M., Kelly, A.J., and Jahn, R.G., "Energy Deposition in Low-Power Coaxial Plasma Thrusters," Journal of Propulsion and Power, Vol. 7, No. 5, September - October 1991, pp. 732-739.

44. LaPointe, M.R., "Numerical Simulation of Geometric Scale Effects in Cylindrical Self-Field MPD Thrusters," AIAA Paper 92-3297, July 1992, see also NASA CR-189224.

45. Choueiri, E.Y., "Electron-Ion Streaming Instabilities of an Electromagnetically Accelerated Plasma," Ph.D. Dissertation, Mechanical and Aerospace Engineering Dept., Princeton University, Princeton, NJ, October 1991.

46. Caldo, G., Choueiri, E.Y., Kelly, A.J., and Jahn, R.G.,"Numerical Simulation of MPD Thruster Flows with Anomalous Transport," AIAA Paper 92-3738, July 1992.

47. LaPointe, M.R., "Numerical Study of Cathode Emission Constraints on Cylindrical, Self-Field MPD Thruster Performance," 10th Symposium on Space Nuclear Power and Propulsion, AIP Proceedings No. 271, January 1993, pp. 1447-1458, NASA CR-190795.

48. Krulle, G., "Theoretical Treatment of Current, Mass Flow, and Related Distribtuions in MPD Plumes," AIAA Paper 72-501, May 1972.

49. Fradkin, D.B., "Analysis of Acceleration Mechanisms and Performance of an Applied-Field MPD Arcjet," Ph.D. dissertation, Princeton University, Dept. of Aerospace and Mechanical Sciences, March 1973.

50. Tanaka, M. and Kimura, I., "Current Distribution and Plasma Acceleration in MPD Arcjets with Applied Magnetic Fields," Journal of Propulsion and Power, Vol. 4, No. 5, September - October 1988, pp. 428-436.

51. Sasoh, A. and Arakawa, Y., "Thrust Formula for an Applied-Field MPD Thruster Derived from Energy Conservation Equation," IEPC Paper 91-062, 22nd International Electric Propulsion Conference, Viarregio, Italy, October 1991.

52. Myers, R.M., "Geometric Effects in Applied-Field MPD Thrusters," AIAA Paper 90-2669, July 1990.

53. Mikellides, P. and Turchi, P.J., "Application of the MACH2 Code to Magnetoplasmadynamic Arcjets," AIAA Paper 92-3740, July 1992.

54. Gilland, J.H., Kelly, A.J., and Jahn, R.G., "MPD Thruster Scaling," AIAA Paper 87-0997, May 1987.

55. Tahara, H., Yasui, H., Kagaya, Y., and Yoshikawa, T., "Experimental and Theoretical Researches on Arc Structure in a Self-Field Thruster," AIAA Paper 87-1093, May 1987.

56. Sleziona, P.C., Auweter-Kurtz, M., and Schrade, H.O., "Numerical Evaluation of MPD Thrusters," AIAA Paper 90-2602, July 1990.

57. Myers, R.M., "Applied-Field MPD Thruster Geometry Effects," AIAA Paper 91-2342, July 1991, see also NASA CR 187163.

58. Myers, R. M., "Scaling of 100 kW Class Applied-Field MPD Thrusters," AIAA Paper 92-3462, July 1992, see also NASA CR 190791.

59. Polk, J.E. and Pivorotto, T.J., "Alkali Metal Propellants for MPD Thrusters," AIAA Paper 91-3572, September 1991.

60. Tahara, H., Kagaya, Y., and Yoshikawa, T., "Hybrid MPD Thruster with Axial and Cusp Magnetic Fields," IEPC Paper 88-058, 20th International Electric Propulsion Conference, Garmish-Partenkirchen, Germany, October 1988.

61. Myers, R.M. and Soulas, G.C. , "Anode Power Deposition in Applied-Field MPD Thrusters," AIAA Paper 92-3463, July 1992, see also NASA CR 190790.

62. Gallimore, A.D., Kelly, A.J., and Jahn, R.G., "Anode Power Deposition in Quasisteady Magnetoplasmadynamic Thrusters," Journal of Propulsion and Power, Vol. 8, No. 6, Nov.-Dec. 1992, pp. 1224 - 1231.

63. Gallimore, A.D., Kelly, A.J., and Jahn, R.G., "Anode Power Deposition in a MPD Thruster with a Manetically Annulled Hall Parameter Anode," AIAA Paper 92-3461, July 1992.

64. Schoenberg, K.F., et al., "Preliminary Investigation of Power Flow and Electrode Phenomena in a Multimegawatt Coaxial Plasma Thruster," AIAA Paper 92-3741, July 1992.

65. Toki, K., Shimizu, Y., and Kuriki, K., "Space Test of 1 kW MPD Thruster System," in Proc. of the 16th International Symp. on Space Technology and Science, 1988, pp. 3 - 8.

66. Polk, J.E., Kelly A.J., and Jahn, R.G., "Characterization of Cold Cathode Erosion Processes," IEPC Paper 88-075, 20th International Electric Propulsion Conference, Garmisch-Partenkirchen, Germany, October 1988.

67. Esker, D.W., Checkley, R.J., and Kroutil, J.C., "Radiation Cooled MPD Arc Thruster," MDC-H296, McDonnell-Douglas Corp., St. Louis, MO, July 1969, see also NASA CR-72557.

68. Ducati, A.C., Muehlberger, E., and Todd, J.P., "Design and Development of a Thermo-Ionic Electric Thrustor," AIAA Paper 64-668, September 1964.

69. Mantenieks, M.A. and Myers, R.M., "Preliminary Test Results of a Hollow Cathode MPD Thruster," IEPC Paper 91-076, 22nd International Electric Propulsion Conference, Viarregio, Italy, October 1991, see also NASA TM 105324.

70. Mantenieks, M.A. and Myers, R.M., "100-kW Class Applied-Field MPD Thruster Component Wear," 10th Symponsium on Space Nuclear Power and Propulsion, AIP Proceedings No. 271, January 1993, pp. 1317-1326.

71. Kuriki, K., Nakamura, K., and Morimoto, S., "MPD Thruster Test on Engineering Test Satellite," AIAA Paper 79-2071, October 1979.

72. Kuriki, K., Morimoto, S., Nakamaru, K., "Flight Performance Test of MPD Thruster System," AIAA Paper 81-0664, April 1981.

73. Kuriki, K., "The MPD Thruster Test on the Space Shuttle," Journal of Spacecraft and Rockets, Vol. 16, No. 5, September-October 1979, pp. 326-332.

74. Kuriki, K., Kawashima, N., Sasaki, S., Yanagisawa, M., and Obayashi, T., "Space Experiment with Particle Acclerators (SEPAC) Performed in Spacelab First," AIAA Paper 85-1996, September 1985.

75. Sazaki, S., et al., "Vehicle Charging Observed in SEPAC Spacelab-1 Experiment," Journal of Spacecraft and Rockets, Vol. 23, No. 2, March-April 1986, pp. 194-199.

76. Sasaki, S., et al., "Neutralization of Beam-Emitting Spacecraft by Plasma Injection," Journal of Spacecraft and Rockets, Vol. 24, No. 3, May-June 1987, pp. 227-199.

77. Ijichi, K., Harada, H., and Kuriki, K., "MPD Arcjet System for Space Experiment with Particle Accelerator (SEPAC)," AIAA Paper 79-2072, October 1979.

78. Kuriki, K., Private Communication, Institute of Space and Astronautical Sciences, Kanagawa, Japan, January 1993.

79. Kuriki, K., "MPD Arcjet System," Japan Society for Aeronautical and Space Sciences Journal, Vol. 33, No. 373, 1985, pp. 89 - 100, translated into NASA TM-88581, February 1987.

80. Kunii, Y., et al., "Verification of Performance and Endurance of Capacitor Bank for the Electric Propulsion Experiment (EPEX)," IEPC Paper 88-048, 20th International Electric Propulsion Conference, Garmish-Partenkirchen, Germany, October 1988.

81. Toki, K., Shimizu, Y., and Kuriki, K., "Development of Repetitively Pulsed Quasi-Steady MPD Thruster," in Proc. of the 15th International Symp. on Space Technology and Science, 1986, pp. 139 - 144.

82. Toki, K, Shimizu, Y., Kuriki, K., Suzuki, H., and Kunii, Y., "The MPD Arcjet thruster System for Electric Propulsion Experiment Onboard Space Flyer Unit," in Proc. of the 17th International Symp. on Space Technology and Science, 1990, pp. 347 - 354.

83. Toki, K, Shimizu, Y., Kuriki, K., Suzuki, H., and Kunii, Y., "Electric Propulsion Experiment (EPEX) Onboard Space Flyer Unit (SFU)," in Proc. of the 18th International Symp. on Space Technology and Science, 1992, pp. 391 - 396.

84. Shiina, K, Suzuki, H., Uematsu, K., Ohtsuka, T., and Toki, K., "Development of MPD Thruster EM for a Space Test," AIAA Paper 90-2558, July 1990.

85. Shimizu, Y., et al., "Development of MPD Arcjet System EM for SFU-1," IEPC Paper 91-147, 22nd International Electric Propulsion Conference, Viarregio, Italy, October 1991.

86. Okamura, T., et al., "Development of the Charge Control Unit for Electric Propulsion Experiment (EPEX), AIAA Paper 90-2626, July 1990.

87. Miller, G.E. and Kelly, A.J., "Hydrogen Performance Measurements," in Electric Propulsion Laboratory Progress Report MAE 1776.38, Princeton University, Dept. of Mechanical and Aerospace Engineering, July-August 1992.

88. Metcalf, K.J., "Multimegawatt Dynamic NEP PMAD Study," 10th Symposium on Space Nuclear Power and Propulsion, AIP Proceedings 271, January 1993, pp. 1197 - 1202.

89. King, D.Q., "100 kWe MPD Thruster System Design," AIAA Paper 82-1897, November 1982.

90. Dailey, C.L. and Lovberg, R.H., "Pulsed Inductive Thruster Performance Data Base for Megawatt-Class Engine Applications," 10th Symposium on Space Nuclear Power and Propulsion, AIP Proceedings No. 271, January 1993.

91. Dailey, C.L, "Plasma Properties in an Inductive Pulsed Plasma Accelerator," AIAA Paper 65-637, 1965.

92. Dailey, C. L. and Lovberg, R.H., "Large Diameter Inductive Plasma Thrusters," AIAA Paper 79-2093, October 1979.

93. Dailey, C. L. and Lovberg, R.H., "Pulsed Inductive Thruster Comp/Tech," Final Report for AFRPL Contract No. F04600-82-C-0058, TRW Space and Technology Group, January 1987.

94. Dailey, C.L. and Lovberg, R.H., "Pulsed Inductive Thruster (PIT) Clamped Discharge Evaluation," Final Report for AFRPL Contract No. F49620-87-C-0059, December 1988.

95. Dailey, C.L. and Lovberg, R.H., "The PIT MkV Pulsed Inductive Thruster," Final Report for NASA Contract NAS1-19291, Task 10, NASA Lewis Research Center, December 1992.

| Anode Material | Number of discharges | $I_{ave}$ mN-s | $I_{sp}$, s | Anode erosion per dischg, μg | Cathode erosion per dischg, μg | Anode erosion per total impulse, mg/N-s |
|---|---|---|---|---|---|---|
| Copper | 103,508 | 24.1 | 1660 | 11.99 | 4.36 | 2.214 |
| Graphite | 101,452 | 20.2 | 2180 | 4.59 | 3.17 | 1.012 |
| Thoriated tungsten | 98,148 | 23.3 | 1820 | 40.25 | 4.10 | 7.694 |
| Tantalum | 101,800 | 23.9 | 1800 | 27.72 | 1.76 | 5.171 |
| Tungsten coated copper (.025 cm) | 101,489 | 24.0 | 1810 | 15.16 | 1.55 | 2.812 |
| Arc cast molybdenum | 100,207 | 23.9 | 1780 | 16.93 | 3.48 | 3.158 |
| 25% copper 75% tungsten | 100,953 | 24.0 | 1750 | 27.81 | 3.86 | 5.155 |
| Platinum | 95,222 | 23.9 | 1500 | 22.79 | 1.18 | 4.252 |

Table 1 Results of side-feed pulsed plasma thruster anode materials tests done at Fairchild. Adapted from Palumbo.[22]

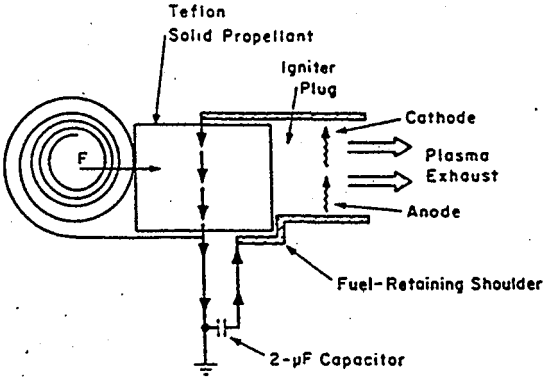


Fig. 1 Pulsed plasma thruster schematic showing teflon feed, spring, discharge region, and current path through the capacitor. Adapted from Vondra et al.[10]

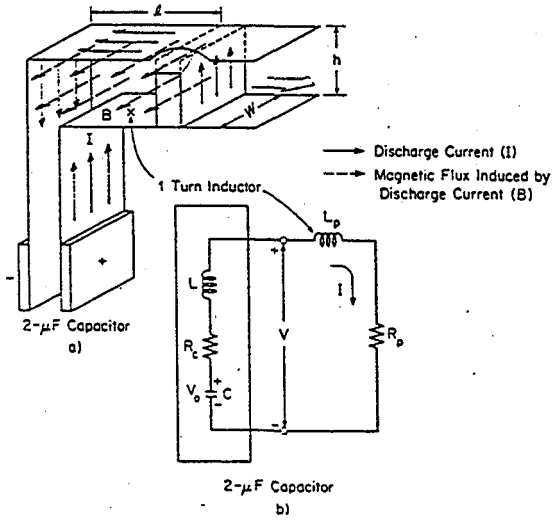


Fig. 2 Schematic of PPT with rectangular electrodes showing the current path, magnetic field, and the plasma arc, and the PPT equivalent circuit. L is the capacitor inductance, $R_c$ is the capacitor resistance, $L_p$ is the time-varying inductance from the moving arc, and $R_p$ is the time-varying plasma resistance. Adapted from Vondra et al.[10]

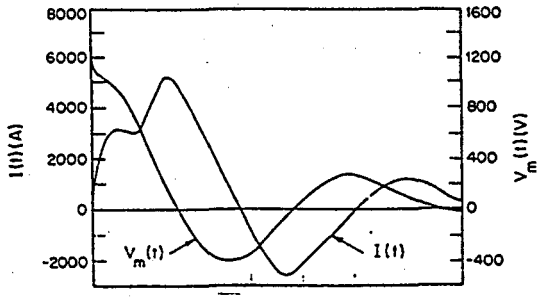


a) Measured PPT voltage, $V_m$, and current, I, waveforms.

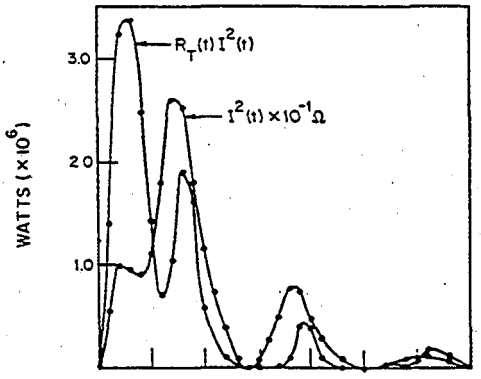


b) Total power, $R_tI^2$, and accelerating magnetic pressure (proportional to $I^2$) waveforms.

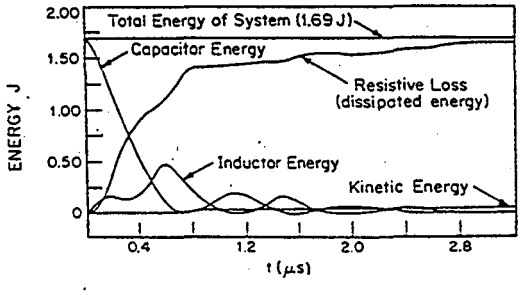


c) Total power distribution.

Fig. 3 Measured PPT discharge characteristics. Adapted from Vondra et al.[10]

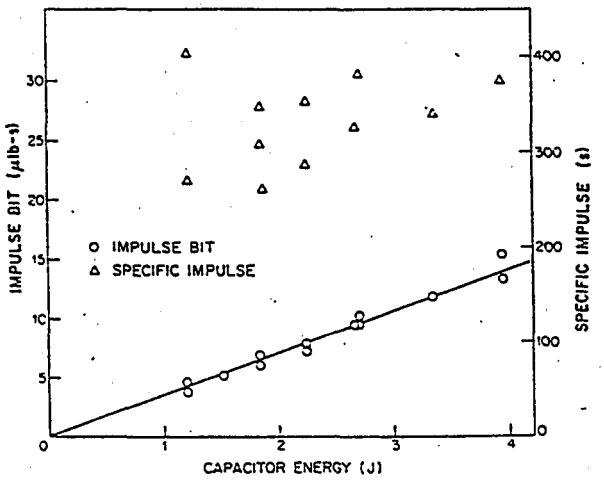


Fig. 4 PPT specific impulse and impulse bit per discharge vs. stored capacitor energy. Adapted from Vondra et al.[10]

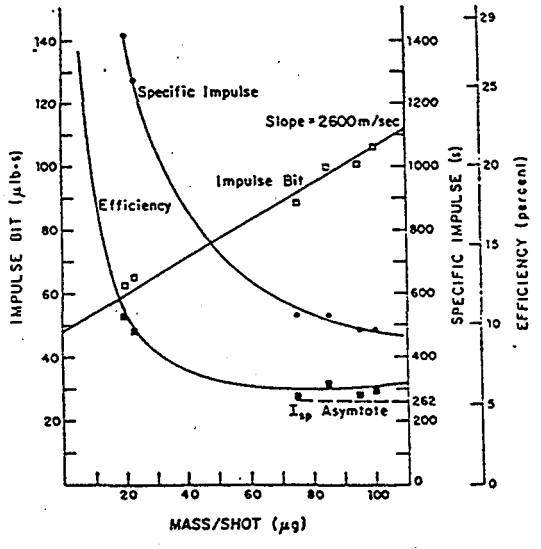


Fig. 5 Performance of 20-joule side-feed PPT with flared electrodes as a function of mass ablated per discharge. Adapted from Vondra and Thomassen.[17]

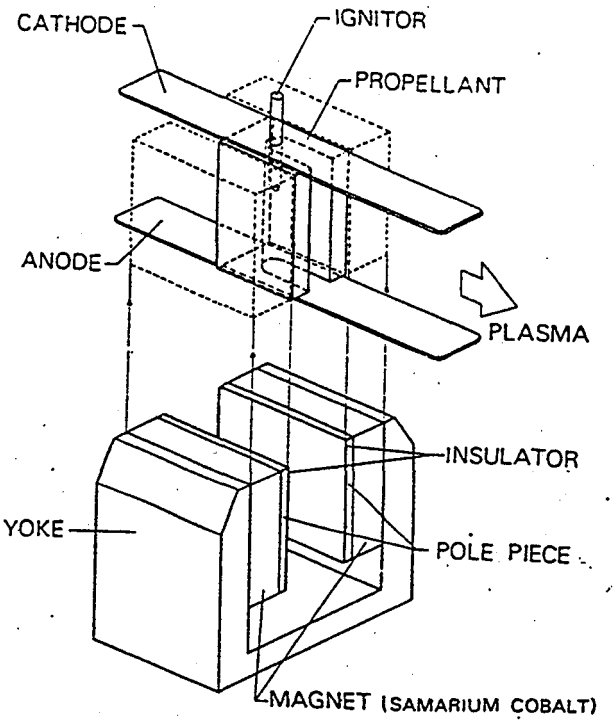


Fig. 6 Applied-field pulsed plasma thruster schematic. Note propellant shape around ignitor. Adapted from Takegahara et al.[19]

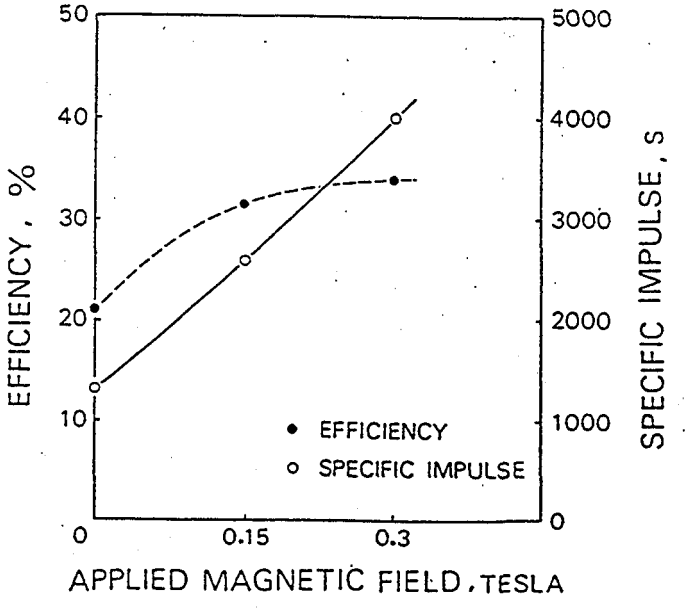


Fig. 7 Efficiency and specific impulse vs. applied magnetic field strength for teflon PPT. Adapted from Takegahara et al.[19]

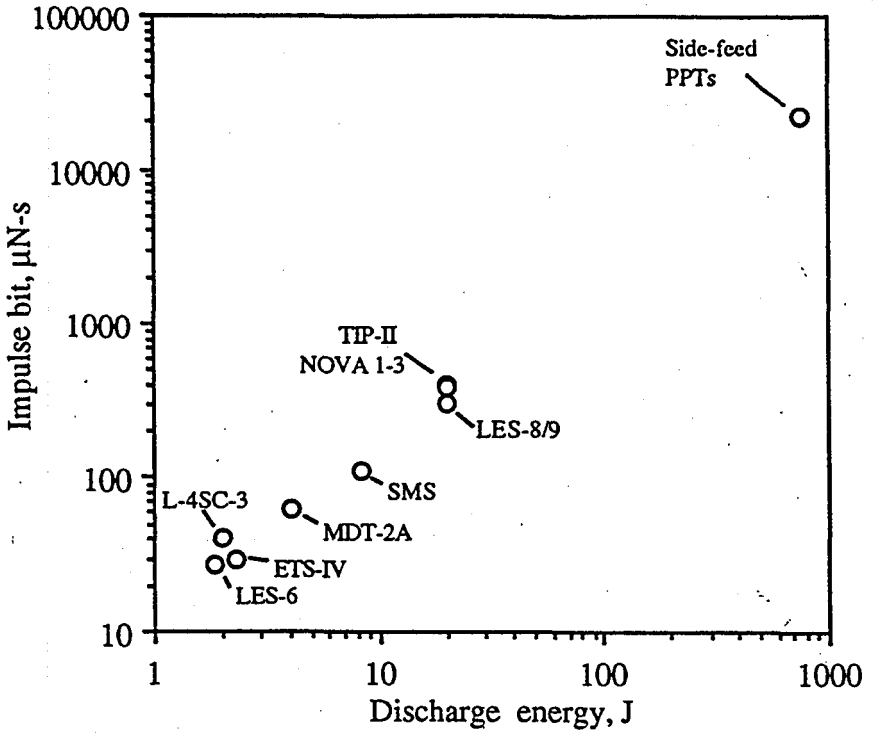


Fig. 8 PPT impulse bit per discharge vs. discharge energy for a variety of space tests.

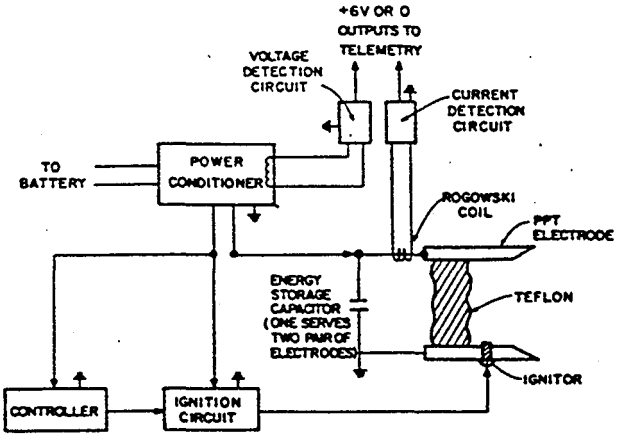


Fig. 9 Schematic of flight PPT system used on Chinese MDT-2A spacecraft. Adapted from An.[6]

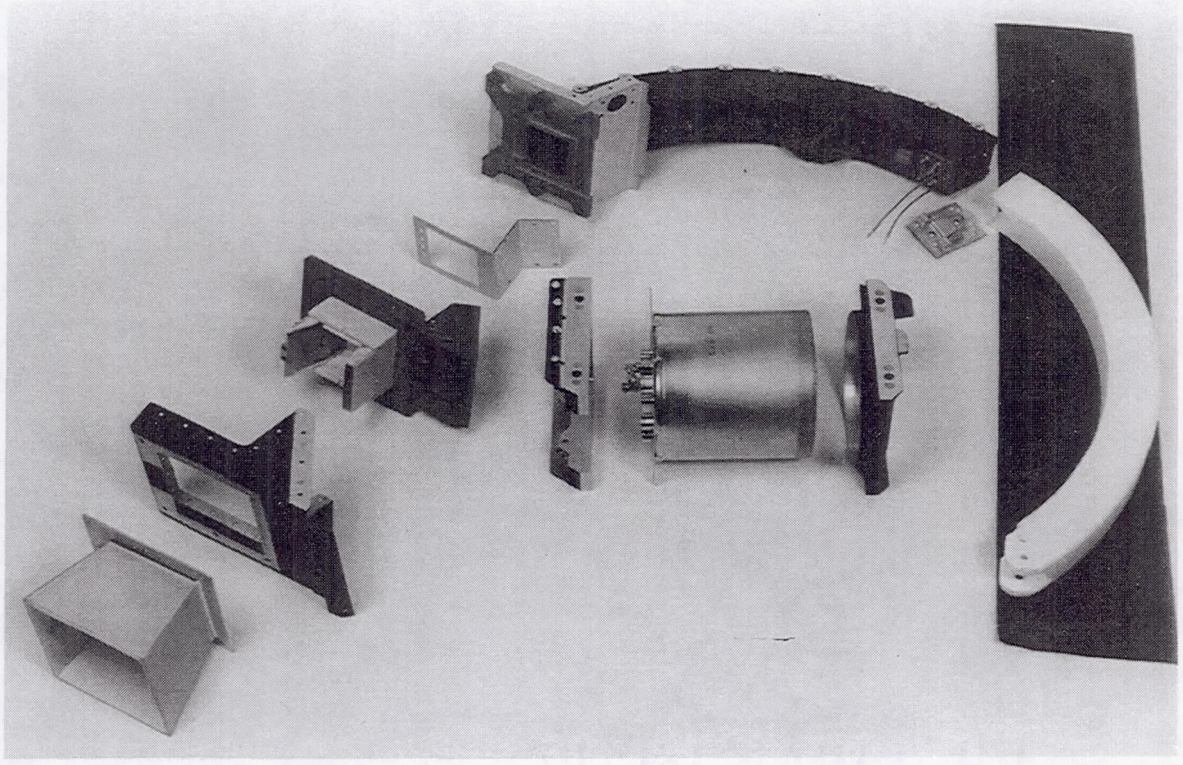

Fig. 10 Component breakdown of the flourinated polymer PPTs used on the NOVA spacecraft. Adapted from Brill et al.[4]

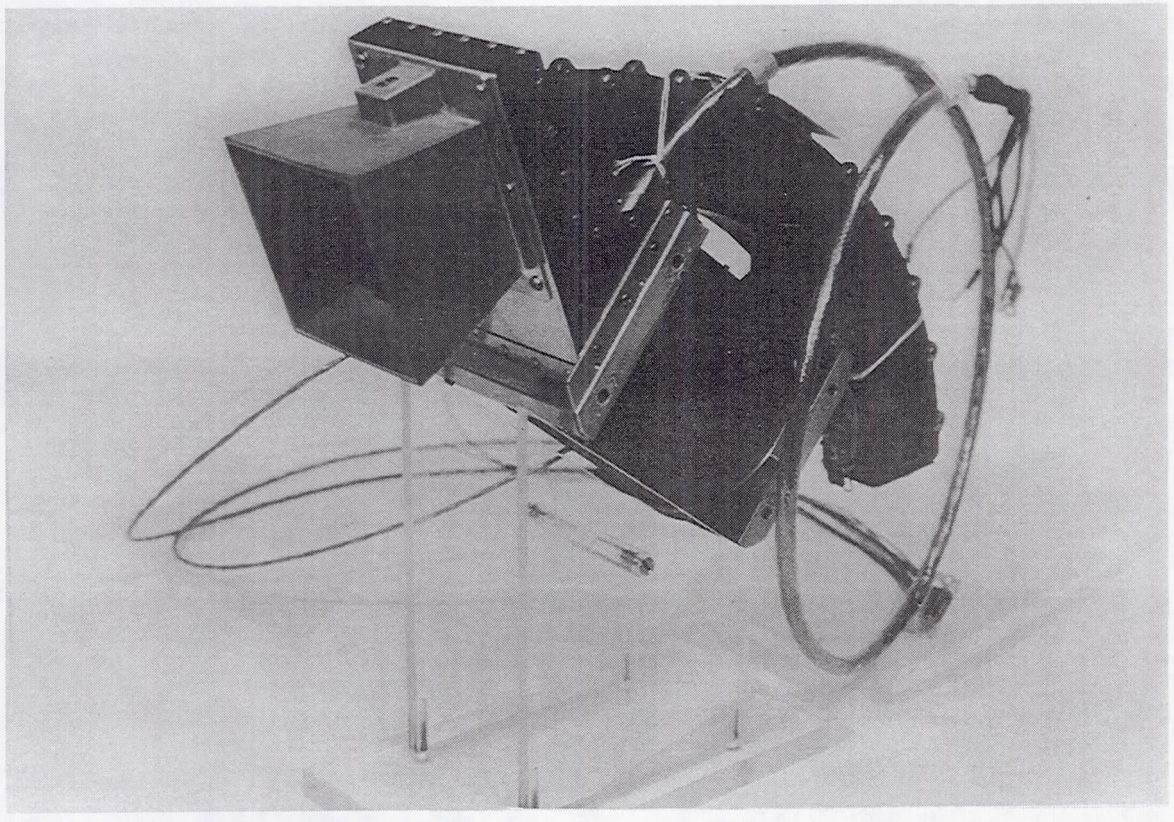

Fig. 11 Flight PPT assembly used on NOVA spacecraft. Adapted from Brill et al.[4]

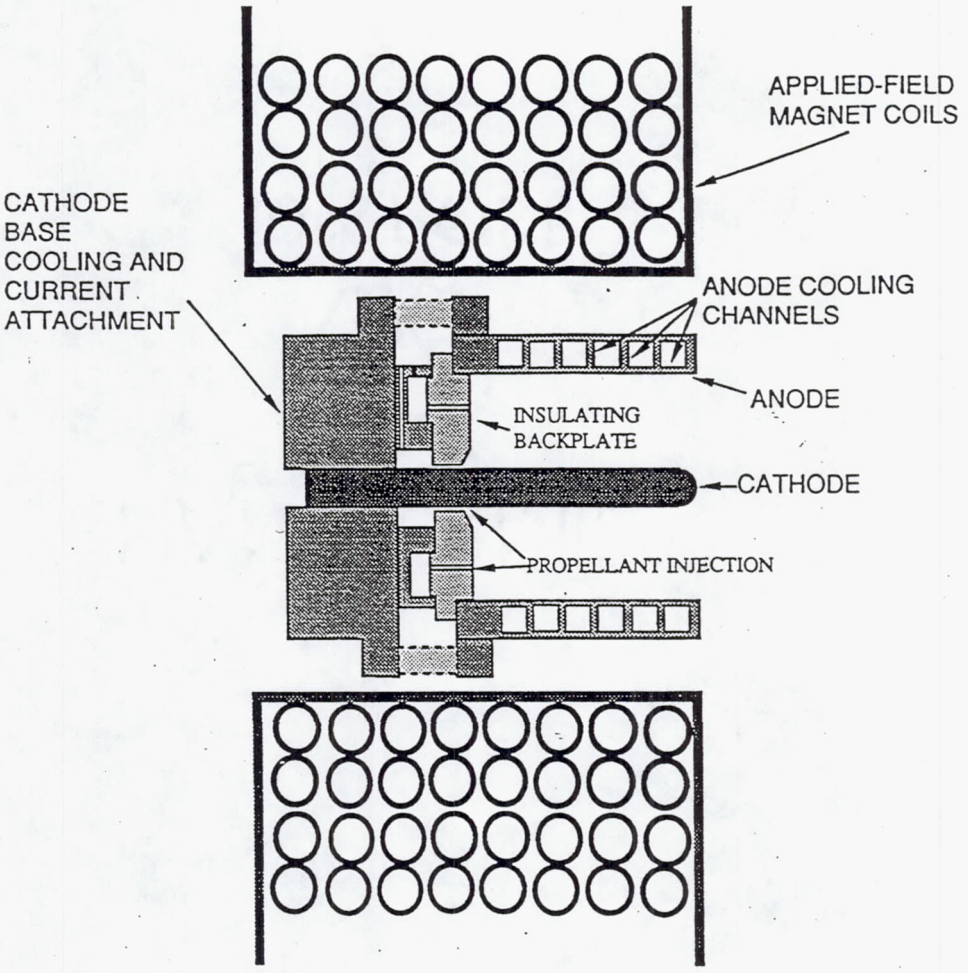


Fig. 12 Applied-field MPD thruster schematic. Adapted from Myers et al.[9]

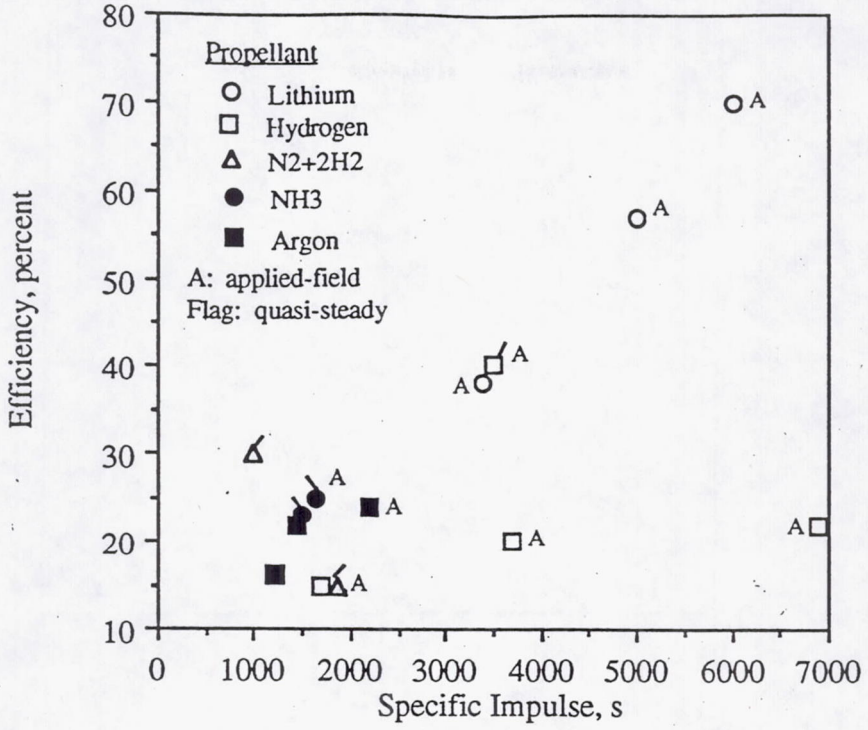


Fig. 13 Peak efficiency - specific impulse values for MPD thrusters. Adapted from Sovey and Mantenieks[8] and Myers, et al.[9]

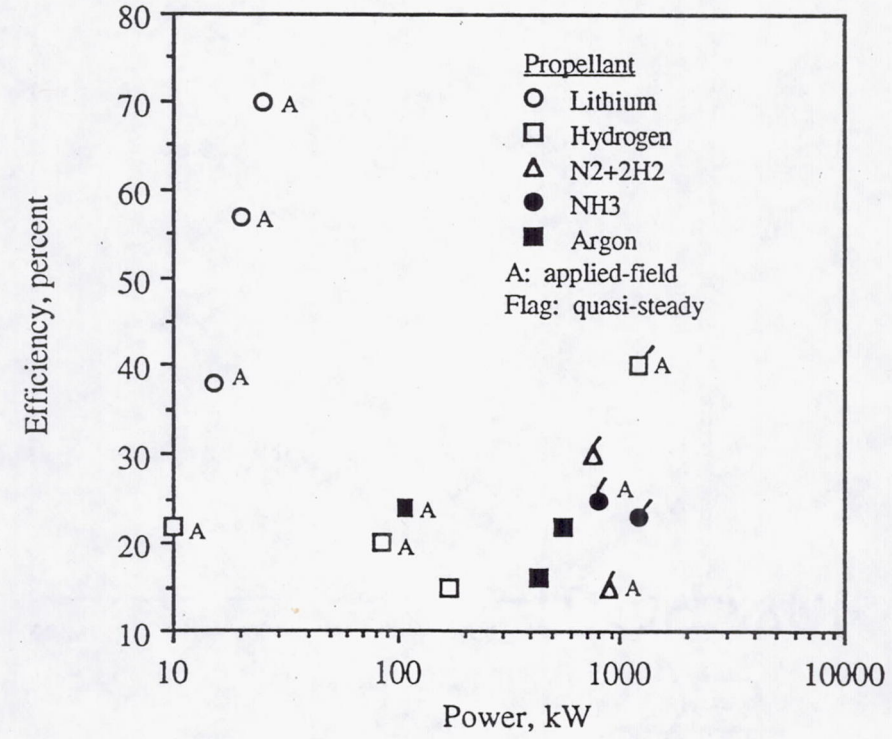


Fig. 14 Peak efficiencies vs. thruster power levels for MPD thrusters. Adapted from Sovey and Mantenieks[8] and Myers, et al.[9]

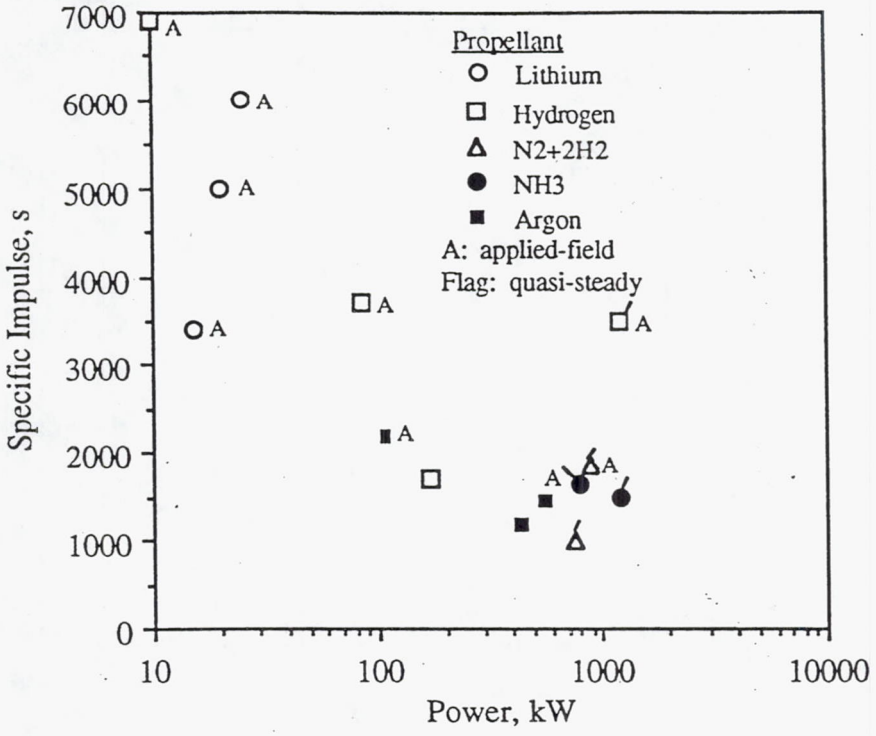


Fig. 15 Peak specific impulses vs. thruster power levels for MPD thrusters. Adapted from Sovey and Mantenieks[8] and Myers, et al.[9]

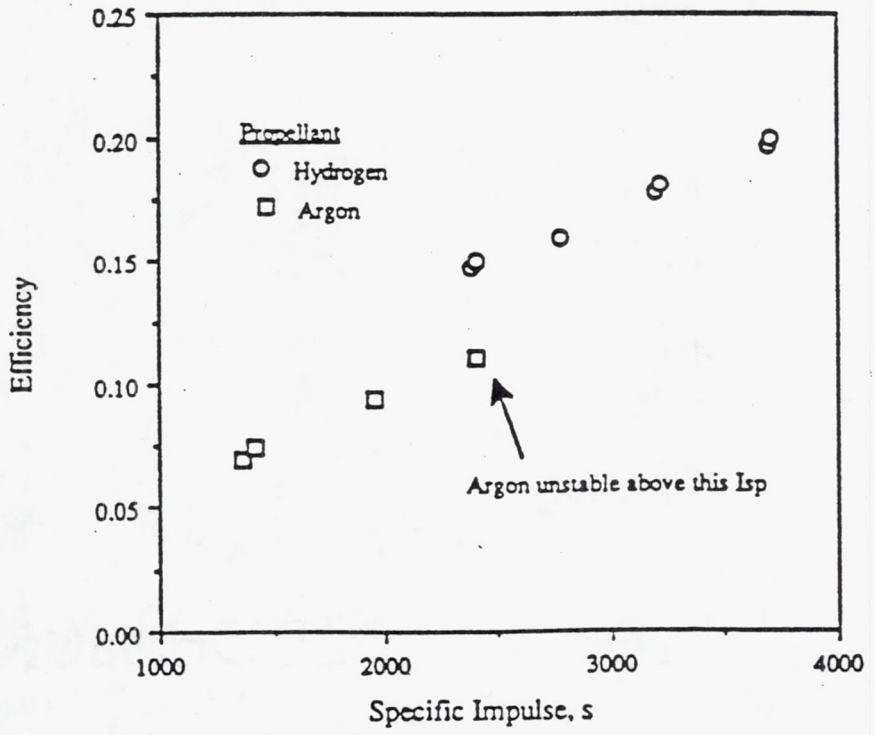


Fig. 16 Comparison of MPD performance levels with argon and hydrogen propellants. Propellant flow rate of 25 mg/s, thruster geometry shown in Fig. 12. Adapted from Myers.[57]

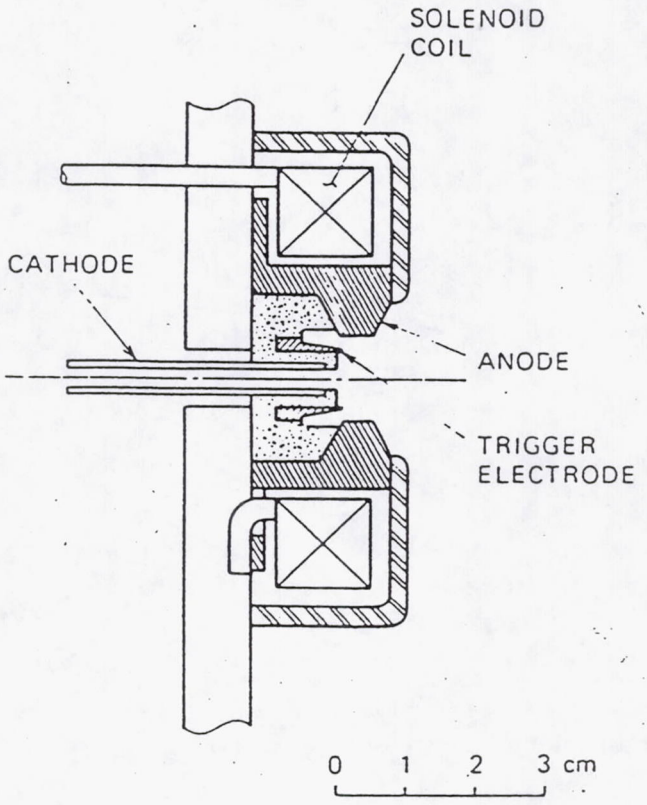


Fig. 17 Schematic of applied-field MPD thruster flown on the Japanese MS-T4 spacecraft. Adapted from Kuriki et al.[71]

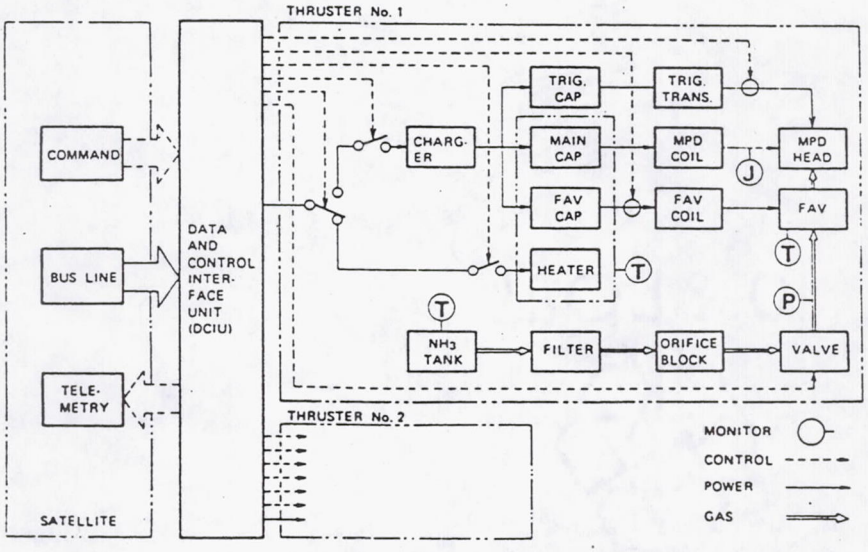


Fig. 18 Flight MPD thruster system schematic for the MS-T4 spacecraft: TRIG = trigger, CAP = capacitor, TRANS = transformer, FAV = Fast acting propellant valve. Adapted from Kuriki et al.[71]

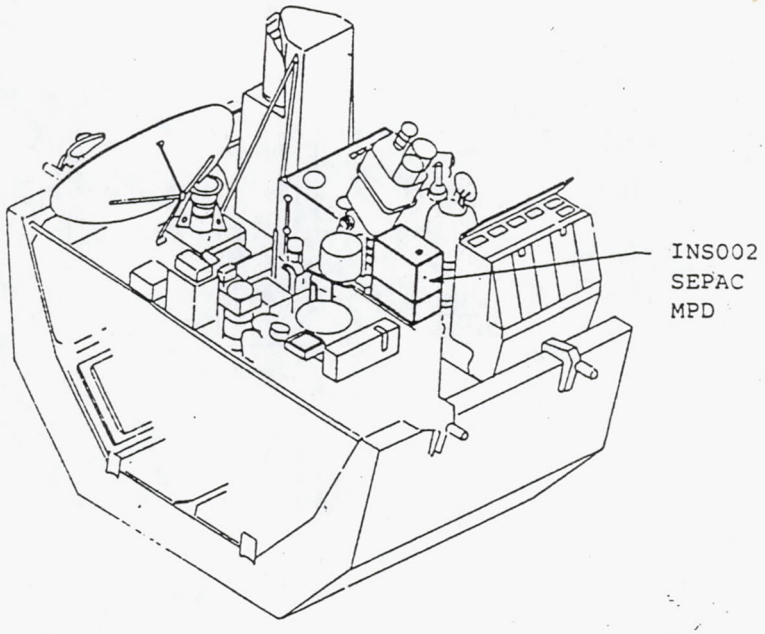


Fig. 19 SEPAC self-field MPD thruster flight experiment mounted on Space Shuttle Spacelab 1 pallet. Adapted from Kuriki et al.[74]

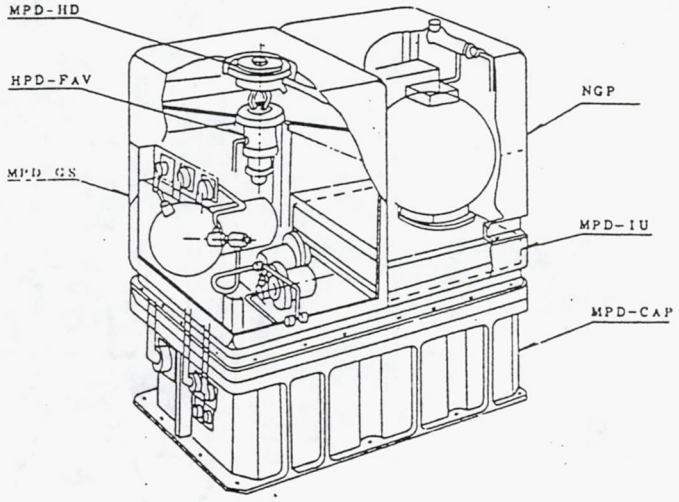


Fig. 20 MPD thruster system mechanical structure: MPD-HD = MPD thruster head, MPD-FAV = MPD fast acting valve, MPD-GS = MPD gas system, MPD-IU = MPD interface unit, MPD-CAP = MPD capacitor bank. NGP was not part of the MPD thruster system. Adapted from Kuriki et al.[74]

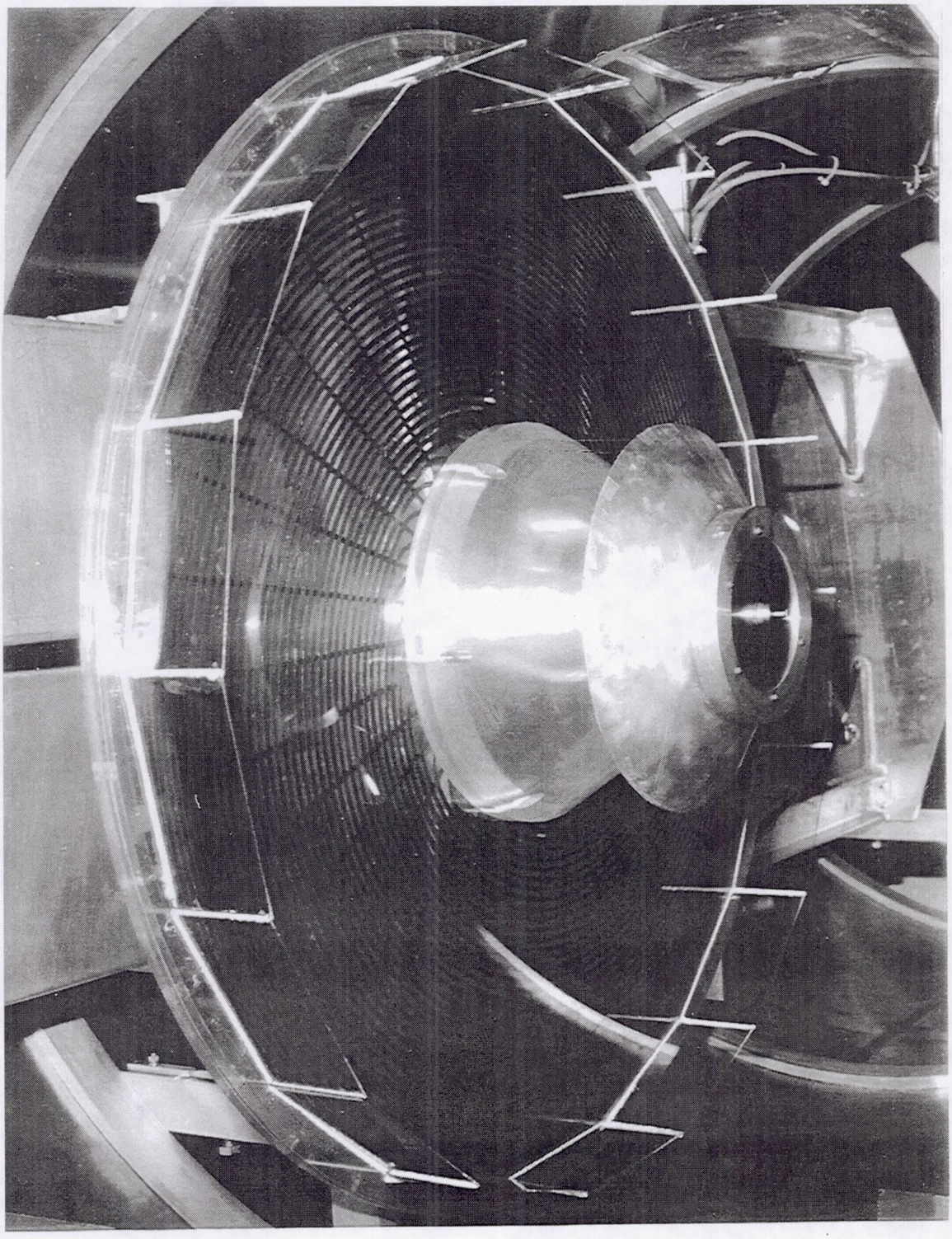

Fig. 21 Mark Va 1 meter diameter pulsed inductive thruster on work stand.
Adapted from Dailey and Lovberg.[95]

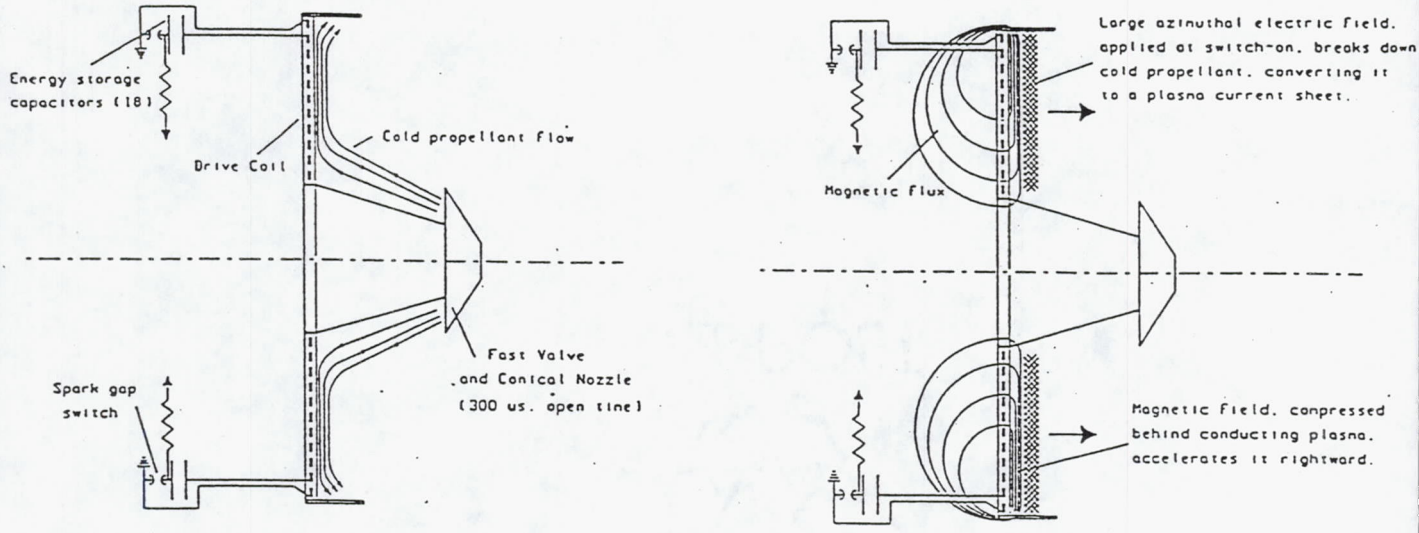


a. Propellant injection and distribution.

b. Magnetic field and plasma current during acceleration.

Fig. 22 PIT thruster schematic and operation. Adapted from Dailey and Lovberg.[95]

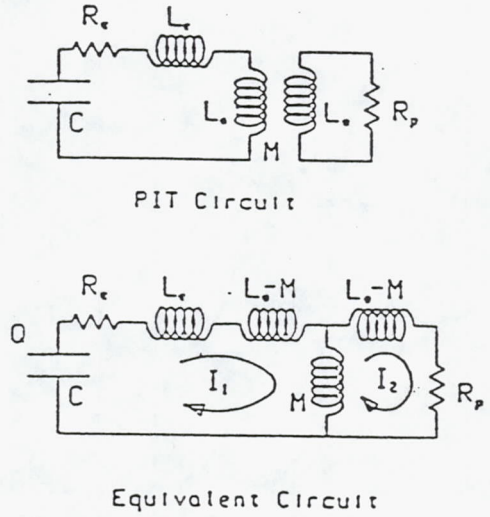


Fig. 23 PIT electrical circuit and its equivalent circuit.
Adapted from Dailey and Lovberg.[95]

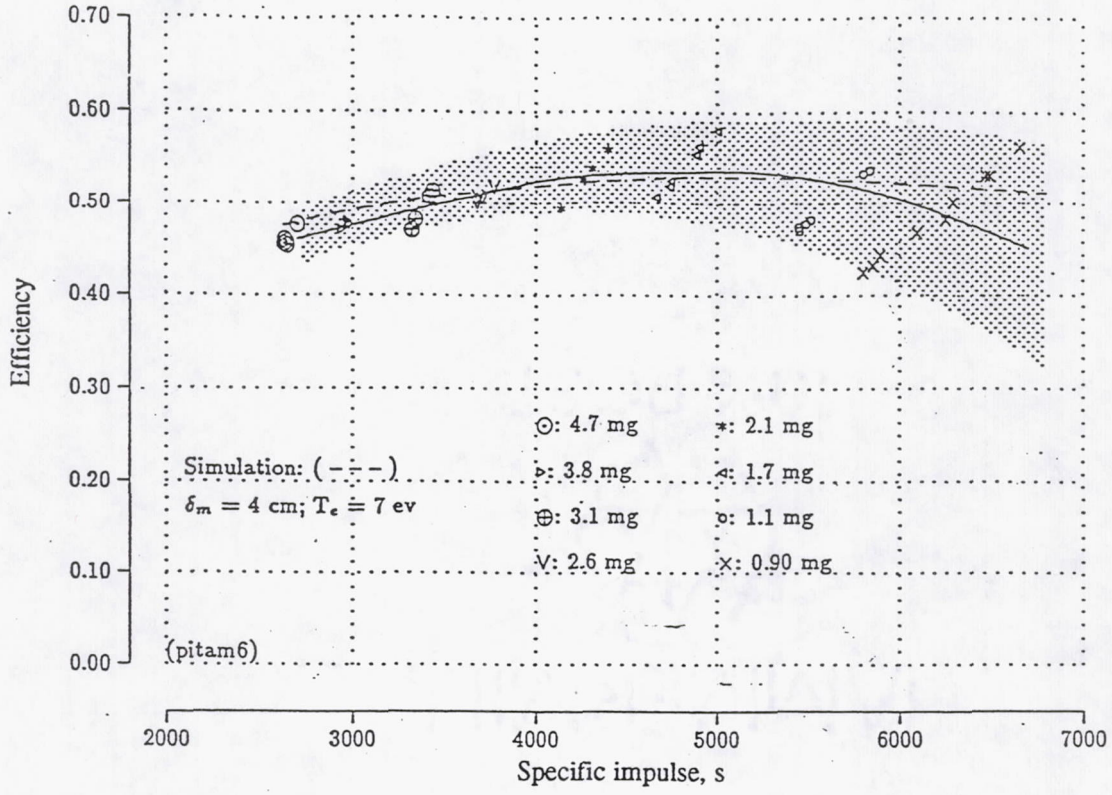


a) Capacitor charging voltage of 14 kV.

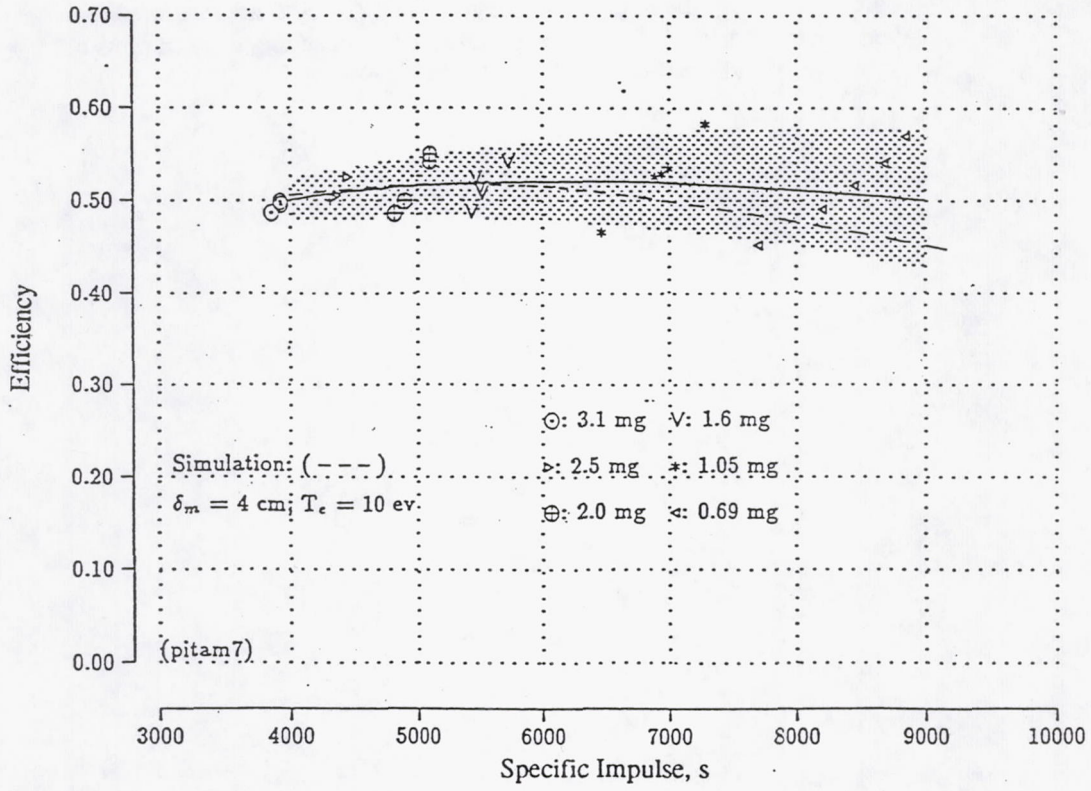


b) Capacitor charging voltage of 16 kV.

Fig. 24 Efficiency vs. specific impulse for PIT Mark Va operating on ammonia propellant. Points are measured data, dashed line is simulation. Specific impulse varied by changing injected propellantmass per pulse. Adapted from Dailey and Lovberg.[95]

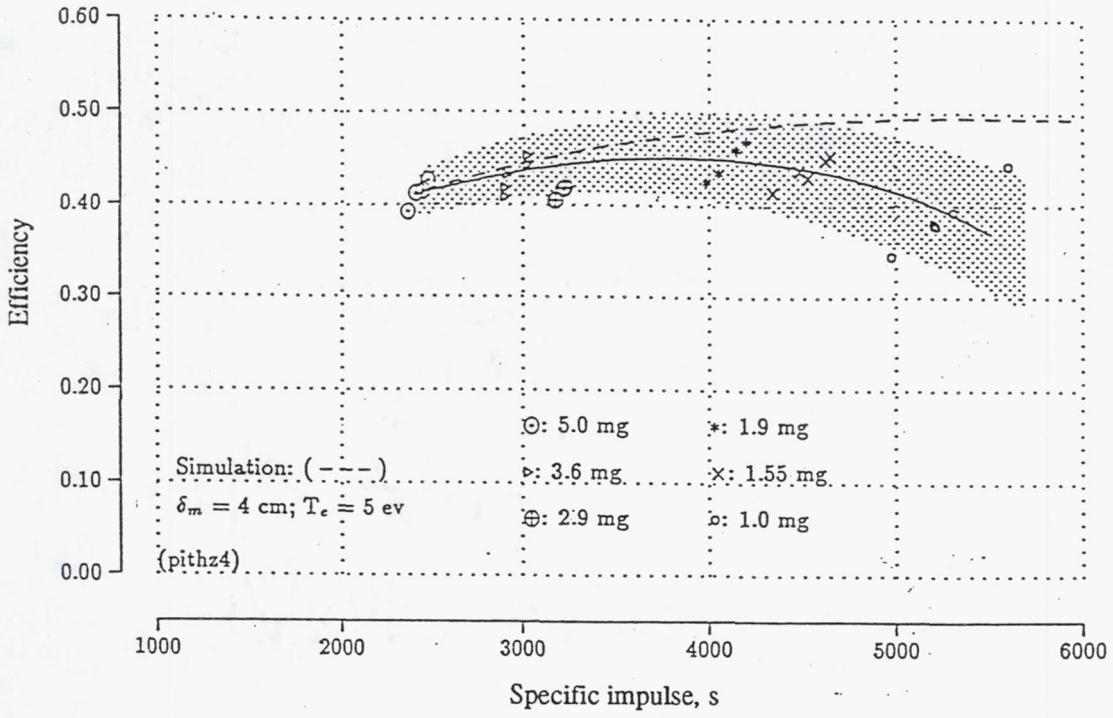


Fig. 25 Efficiency vs. specific impulse for PIT Mark Va operating on simulated hydrazine propellant with a capacitor charging voltage of 14 kV. Points are measured data, dashed line is simulation. Specific impulse varied by changing injected propellant mass per pulse. Adapted from Dailey and Lovberg.[95]

# REPORT DOCUMENTATION PAGE

Form Approved
OMB No. 0704-0188



| 1. AGENCY USE ONLY (*Leave blank*) | 2. REPORT DATE | 3. REPORT TYPE AND DATES COVERED |
|---|---|---|
| | September 1993 | Final Contractor Report |

**4. TITLE AND SUBTITLE**

Electromagnetic Propulsion for Spacecraft

**5. FUNDING NUMBERS**

WU–506–42–31
C–NAS3–25266

**6. AUTHOR(S)**

Roger M. Myers

**7. PERFORMING ORGANIZATION NAME(S) AND ADDRESS(ES)**

Sverdrup Technoloyg, Inc.
Lewis Research Center Group
2001 Aerospace Parkway
Brook Park, Ohio 44142

**8. PERFORMING ORGANIZATION REPORT NUMBER**

E–8097

**9. SPONSORING/MONITORING AGENCY NAME(S) AND ADDRESS(ES)**

National Aeronautics and Space Administration
Lewis Research Center
Cleveland, Ohio 44135–3191

**10. SPONSORING/MONITORING AGENCY REPORT NUMBER**

NASA CR–191186
AIAA-93–1086

**11. SUPPLEMENTARY NOTES**

Prepared for the 1993 Aerospace Design Conference, Irvine, California, February 15–18, 1993. Project Manager, James S. Sovey, Space Propulsion Technology Division, (216) 433–7454.

**12a. DISTRIBUTION/AVAILABILITY STATEMENT**

Unclassified - Unlimited
Subject Categories 18, 20, and 75

**12b. DISTRIBUTION CODE**

**13. ABSTRACT** ***(Maximum 200 words)***

Three electromagnetic propulsion technologies, solid propellant pulsed plasma thrusters (PPT), magnetoplasmadynamic (MPD) thrusters, and pulsed inductive thrusters (PIT), have been developed for application to auxiliary and primary spacecraft propulsion. Both the PPT and MPD thrusters have been flown in space, though only PPTs have been used on operational satellites. The performance of operational PPTs is quite poor, providing only ~ 8% efficiency at ~ 1000 s specific impulse. However, laboratory PPTs yielding 34% efficiency at 2000 s specific impulse have been extensively tested, and peak performance levels of 53% efficiency at 5170 s specific impulse have been demonstrated. MPD thrusters have been flown as experiments on the Japanese MS-T4 spacecraft and the Space Shuttle and have been qualified for a flight in 1994. The flight MPD thrusters were pulsed, with a peak performance of 22% efficiency at 2500 s specific impulse using ammonia propellant. Laboratory MPD thrusters have been demonstrated with up to 70% efficiency and 700 s specific impulse using lithium propellant. While the PIT thruster has never been flown, recent performance measurements using ammonia and hydrazine propellants are extremely encouraging, reaching 50% efficiency for specific impulses between 4000 to 8000 s. This paper reviews the fundamental operating principals, performance measurements, and system level design for the three types of electromagnetic thrusters, and available data on flight tests are discussed for the PPT and MPD thrusters.

**14. SUBJECT TERMS**

Electric propulsion; Plasma dynamics

**15. NUMBER OF PAGES**

32

**16. PRICE CODE**

A03

| 17. SECURITY CLASSIFICATION OF REPORT | 18. SECURITY CLASSIFICATION OF THIS PAGE | 19. SECURITY CLASSIFICATION OF ABSTRACT | 20. LIMITATION OF ABSTRACT |
|---|---|---|---|
| Unclassified | Unclassified | Unclassified | |